ANALYSIS OF HORIZONTALLY CURVED GIRDER BRIDGES

by

ANN LOUISE FIECHTL, B.S.C.E.

THESIS

Presented to the Faculty of the Graduate School of

The University of Texas at Austin

in Partial Fulfillment

of the Requirements

for the Degree of

MASTER OF SCIENCE IN ENGINEERING

THE UNIVERSITY OF TEXAS AT AUSTIN

August 1987

ACKNOWLEDGEMENTS

The author wishes to acknowledge, with sincere thanks, the guidance, input, and efforts provided by Dr. Greg L. Fenves, and is indebted to him for the time that he generously devoted as supervising professor. The support of Dr. Karl H. Frank is also appreciated. For his assistance, appreciation is extended also to Kris Hahn, a fellow graduate student. The efforts of those at the Ferguson Structural Engineering Lab involved with the preparation of this thesis are also acknowedged.

TABLE OF CONTENTS

TABLE OF CONTENTS (continued)

LIST OF FIGURES

LIST OF FIGURES (continued)

LIST OF FIGURES (continued)

LIST OF FIGURES (continued)

LIST OF TABLES

CHAPTER 1

INTRODUCTION

1.1 Background and Objectives

The design of todays roadways has become increasingly demanding on the engineer. The use of horizontally curved bridges has grown out of alignment requirements and constraints. The right of way available for the construction of a new roadway may be limited because of the expansion that many cities are experiencing. It may be impossible to build a straight bridge or overpass, so an alternate design is necessary with the bridge alignment adapted to suit the area.

In addition to designing a bridge to suit the site, the spans can be continuous which allows shallower girders. The aesthetics of a curved bridge is also an advantage. There are, however, disadvantages which the designer should be aware of when using curved bridges. The fabrication costs are generally larger, and the curved bridge segments are produced in smaller pieces which increases the erection and transportation costs. Analysis of curved bridges is different than a straight bridge due to the twisting of the unit due to its curvature.

The objective of this research is to develop and implement an approximate method of analysis for horizontally curved bridge units. Bending and warping stresses and the

envelope responses of bending moment, shear force, and reactions are computed. The effects of the design parameters on the response quantities are evaluated, and the accuracy of the approximate method is assessed by comparison of the results to those of a more exact analysis.

1.2 Review of Previous Work

One of the first presentations of an approximate analysis of horizontally curved girders was by the United States Steel Corporation in 1963 (11,13,14). This report analyzed a two girder curved bridge using an approximate method along with a verification of its results using a rigorous indeterminate analysis (13,14). About the same time, Dabrowski (12) developed expressions for the warping moment in a curved girder using differential equations.

The United States Steel approximate method became known as the V-load method and was extended to be applicable to multigirder bridge units in 1965 (13). A computer program was developed using this method in 1966 and made available to engineers for multigirder bridge units with radial supports (13).

Developments were also made by Gillespie and Ketchek. Gillespie (5) used an approximate analysis method in which he found that the lateral bending stress was dependent on the lateral bending moment which is related to the diaphragm spacing.

Another method was developed by Ketchek (11) who, in addition to allowing for the V-loads used in earlier reports, allowed for the direct application of uniformly distributed torsional moments to the girders.

In the 1970's, CURT, Consortium of University Research Teams (2,13), was established to develop methods of curved bridge design and analysis and determine bridge requirements. Also during this time, Weissman (18) was developing a method for curved girders using statically indeterminate analysis of plane grid systems with straight elements. The slope deflection technique was used by Heins and Siminou (9) to determine various distribution factors to relate a single straight girder to a single curved girder and then to a curved system of girders.

Culver, Brogan, and Bednar (3) utilized the flexibility method and flexibility coefficients derived by Dabrowski to develop an approximate analysis using equivalent straight girders. They discovered that the maximum deflection of a curved girder is much larger than that of an equivalent straight girder. For small radii of curvature a curved beam is more flexible than the equivalent straight girder, and the ratio of deflections between a curved and a straight girder increases as the radius of curvature decreases. They also found that the diaphragm spacing influenced the maximum warping stress but not the bending stress.

The approximate method predicted the outer girder stress fairly well but underestimated the stress on the inner girder (3).

Heins and Spates (10) developed a computer program using differential equations with reasonable experimental correlation for the response of a single curved girder subjected to various loadings and boundary conditions.

In the 1980's the V-load method was revised to accomodate skewed bridges with the effort of US Steel Research and Richardson, Gordon, and Associates (13,15,16). Grubb (6) found this approximate analysis method very accurate for the dead load condition. For live load he found that the V-load results were reasonable for the exterior girders but not for the interior girders. The correlation was largely influenced by the lateral distribution factors assumed in the V-load method.

Heins and Jin (8) in 1984 developed expressions for live load distribution factors for braced systems by the use of a three-dimensional space frame matrix formulation. Bottom bracing was added to their models to examine its effect on the load distribution. Bracing stiffens the system and the live load is distributed more uniformly to all the girders and the load to a given girder is decreased.

1.3 Organization of Report

This report is comprised of Chapters 1 through 6. The chapters explain the theory, use, and accuracy of the approximate V-load analysis method.

In Chapter 2 the fundamentals of the approximate V-load analysis are described for both a two girder and multigirder bridge unit. The theory behind using equivalent straight girders to compute the bending and warping stresses will be explained. Chapter 3 describes the analysis procedures used to compute the response of a bridge unit to a single load, a girder to a single load, response envelopes, and the warping stresses which develop in the flanges. Chapter 4 presents the V-load reponses of a two girder and multigirder bridge units. The same bridge configurations are analyzed by a finite element method and the V-load and finite element responses compared. The affect of the radius of curvature, diaphragm spacing, and support orientation on the responses will be determined. Chapter 5 presents the bending moment, shear force, and reaction envelopes due to a truck load moving along two bridge units. Lateral distribution factors for the live load are included in the response computations. Chapter 6 summarizes the approximate V-load analysis method and presents conclusions drawn during this study.

CHAPTER 2

APPROXIMATE ANALYSIS OF HORIZONTALLY CURVED BRIDGES

2.1 Introduction

Horizontally curved bridges respond to loads differently than do straight bridges because torsional forces attempt to rotate the bridge about the longitudinal axis. An approximate method of analysis for horizontally curved bridges can be developed using equivalent straight girders if the torque produced by the curvature of the girders is represented by self-equilibrating loads on the girders. These additional loads are called V-loads because they are a set of vertical shears on the equivalent straight girders. The V-loads are developed from equilibrium requirements and are primarily a function of the radius of curvature, width of the bridge unit, and spacing of diaphragms between the girders.

This chapter presents the V-load method for approximate analysis of horizontally curved bridge units. The development closely follows References 5, 6, 13 and 15. The method will first be developed for a two girder bridge unit and then for a multigirder bridge unit.

2.2 Two Girder Bridge Unit

The approximate forces on two horizontally curved girders connected with radial diaphragms can be determined from

equilibrium. Figure 2.1 shows a horizontally curved bridge unit with two girders spaced a distance D. The angle of curvature of the bridge is θ. The radius to the outside girder, girder 1, is shown as R_1 and the arclength of girder 1 is L_1. The radius and arclength of girder 2 are R_2 and L_2 respectively. Radial diaphragms, with spacing d, connect girders 1 and 2.

Vertical loads on the bridge produce bending moments in both girders. Assuming the plate girder sections resist the bending moment by longitudinal forces in the flanges, as shown in Fig. 2.2, the force in each flange of girder 1 is M_1/h_1, where h_1 is the depth of the girder and M_1 is the bending moment. In girder 2 the bending moment is M_2 and the flange forces are M_2/h_2. However, because the flanges of the girder are horizontally curved, the longitudinal forces due to bending are not in equilibrium. Figure 2.3 shows a section of the top flange of girder 1 centered about a diaphragm, where the longitudinal forces due to bending are not colinear. To maintain radial equilibrium of the flange, the chord of the diaphragm must develop a force. Figure 2.4 shows a freebody diagram of a diaphragm between the girders.

The force, H_1, which develops in the diaphragm is found by equilibrium along a radial line at the diaphragm

location. Referring to Fig. 2.3 the force H_1 is :

$$H_1 = \frac{M_1 \theta}{h_1} \tag{2.1}$$

Substituting the geometrical relationship $\theta = d_1/R_1$, where d_1 is the diaphragm spacing of girder 1, into Eq. 2.1 gives :

$$H_1 = \frac{M_1 d_1}{h_1 R_1} \tag{2.2}$$

The corresponding diaphragm force H_2 for girder 2 is computed using the same procedure as used for H_1. The direction of H_2 is opposite that of H_1 because girder 2 is on the inside of the bridge unit. Because of the forces on the chords of the diaphragm, a vertical shear is required for equilibrium of the diaphragms as shown in Fig. 2.4. For moment equilibrium of the diaphragm the vertical shear is :

$$V = (H_1 + H_2) \frac{h}{D} \tag{2.3}$$

where the two girders are assumed to have the same depth h.

Substituting Eq. 2.2 for H_1 and a similar expression for H_2 into Eq. 2.3 gives :

$$V = \frac{M_1 \, d_1/R_1 + M_2 \, d_2/R_2}{D}$$

But from geometry, $d_1/R_1 = d_2/R_2 = d/R$, so the shear force

in the diaphragm is :

$$V = \frac{M_1 + M_2}{R\ D/d} \tag{2.4}$$

These shear forces in the diaphragm act in the opposite direction on girders 1 and 2 (Fig. 2.4). The shear forces, known as V-loads, are self-equilibrating forces on the bridge unit that approximate the effects of the horizontal curvature of the girders. They must be self-equilibrating forces because they are not actual loads applied to the bridge unit.

The bending moments M_1 and M_2 are the moments in girders 1 and 2 due to the applied loads and the additional forces due to curvature , as represented by the V-loads. The two contributions to the totals moment can be separated as :

$$M_1 = M_{1p} + M_{1v} \tag{2.5}$$

$$M_2 = M_{2p} + M_{2v} \tag{2.6}$$

The subscripts p and v denote responses due to the P-loads, which are applied loads, and V-loads respectively.

In common application of the V-load method (15), the bending moments produced by the V-loads are assumed proportional to their respective girder lengths :

$$\frac{M_{2v}}{L_2} = \frac{-M_{1v}}{L_1}$$

Substituting this relationship into Eqs. 2.5 and 2.6 and summing M_1 and M_2 gives :

$$M_1 + M_2 = M_{1p} + M_{2p} + (M_1 * (1 - \frac{L_2}{L_1})) \qquad (2.7)$$

In Eq. 2.7, the quantity L_2/L_1 is generally close to 1 so $(1 - L_2/L_1)$ is small. Consequently, total bending moments may be approximated by P-loads only. With this simplification, Eq. 2.4 gives the magnitude of the V-loads as a function of the P-load moments only :

$$V = \frac{M_{1p}+M_{2p}}{R\ D/d} \qquad (2.8)$$

In summary, the V-load method involves analyzing equivalent straight girders twice. The first analysis gives the response to P-loads, including M_{1p} and M_{2p}. The second analysis gives the response to the self-equilibrating V-loads. The total response on the girders is the sum of the response to the P-loads and V-loads.

2.3 Multiple Girder Bridges

In a curved bridge unit with two girders, the outer girder sees an increase in load due to the curvature while the inner one sees a decrease in load. Up to the computation of the diaphragm forces and the corresponding V-loads on the girders, the analysis procedure is not dependent on the number of girders

in the unit. A general expression for the V-loads acting on multiple girder units can be developed using the same procedure as for the two girder bridge geometry. Figure 2.5 shows a cross section of a bridge with N_g girders, where D is the distance between outer and inner girders.

Due to the curvature of the unit the section is subjected to twisting. Lateral flange forces develop and produce forces in the diaphragms as described in Sec. 2.2. The V-loads are derived using equilibrium between the girders and the diaphragms. It can be shown that equilibrium of the diaphragm panels allows summation of the lateral flange forces, H_i, in terms of the shear forces in the diaphragm panels:

$$\sum_{i=1}^{N_g} H_i = \sum_{i=1}^{N} V_i' \left(\frac{D}{Nh}\right) \tag{2.9}$$

where V_i' is the shear in diaphragm i, H_i is the lateral flange force in girder i, h is the depth of the girders, and N is the number of diaphragm panels in the cross section, $N=N_g - 1$. As developed in Sec. 2.2, the flange force, H_i, is related to the bending moment in girder i, M_i by :

$$H_i = \frac{M_i d}{hR} \tag{2.10}$$

Substitution of Eq. 2.10 into Eq. 2.9 gives :

$$\sum_{i=1}^{N_g} M_i \frac{dN}{RD} = \sum_{i=1}^{N} V_i' \qquad (2.11)$$

Considering a freebody diagram of the section the shear in panel j, V_j', is equal to the sum of the shear forces on girders 1 to j:

$$V_j' = \sum_{i=1}^{j} V_i \qquad (2.12)$$

where V_i is the force on girder i. Assuming a linear distribution of shear forces on the girders the shear in girder i can also be expressed as :

$$V_i = V \left[1 - \frac{2(i-1)}{N}\right] \qquad (2.13)$$

where V is the shear force on the outermost girders. Combining Eq. 2.12 and 2.13 gives :

$$V_j' = \sum_{i=1}^{j} V\left[1 - \frac{2(i-1)}{N}\right] \qquad (2.14)$$

Substitution of Eq. 2.14 into Eq. 2.12 gives:

$$C'V = \sum_{i=1}^{N_g} M_i \left(\frac{dN}{RD}\right)$$

where

$$C' = \sum_{j=1}^{N} \sum_{i=1}^{j} \left[1 - \frac{2(i-1)}{N}\right] \qquad (2.16)$$

or

$$V = \frac{\sum_{i=1}^{N_g} M_i}{C'(RD/dN)} \qquad (2.17)$$

The difference between this expression for the multi-girder unit and the one for the two girder unit, Eq. 2.4, is the coefficient C' and N. Evaluation of the double summations in Eq. 2.16 gives:

$$C' = 1/2\ (N+1)^2 - 1/6\ (N+1)(2N+1) \qquad (2.18)$$

Defining C = C'/ N, Eq. 2.17 can be written as:

$$V = \frac{\sum_{i=1}^{N_g} M_i}{C(RD/d)} \qquad (2.19)$$

Substituting $N = N_g - 1$ into Eq. 2.18 gives an expression for C in terms of the number of girders in the bridge unit :

$$C = 1/6\ \frac{N_g(N_g+1)}{N_g-1} \qquad (2.20)$$

A check of this expression for a two girder unit gives a value of C equal to 1.0. This is the same coefficient as found in the derivation of the two girder unit. Table 2.1 lists the value of C as a function of the number of girders, N_g.

In summary, the first of two analyses for each equivalent straight girder gives the P-load moment, shear, and reaction responses, M_p, V_p, and R_p respectively. The second analysis gives the responses due to the V-loads. The expression for the V-load factor is dependent on the number of girders as derived above. The V-loads are assumed to be distributed linearly between the outer and inner girders and therefore the V-load on a girder is proportional to its distance from the bridge centerline.

2.4 Torsional Response of Girders

Because of the horizontal curvature of the bridge unit the girders must resist torsional forces. The two types of torsional stresses which can exist in wide flange sections are St. Venant's torsion and warping torsion. The St. Venant stiffness for wide flange girders is much less than its warping stiffness. For this reason, St. Venant's stresses are generally much less than the warping stresses, so St. Venant's torsion is neglected in an approximate analysis of curved girder units without bracing in the plane of the bottom flanges. All of the torsion is assumed to be resisted by warping of the girders. The section of a girder twisted through an angle θ, by a torque, T, is shown in Fig. 2.6. Due to this twisting the flanges deflect laterally a distance x. The torque creates flange shear

forces, T/h, in the direction of the torque, where h is the depth of the plate girder section. These flange shears cause lateral bending moments, M_f, in the flange.

The effects of warping torsion can be approximated by applying lateral forces to a straight model of the bottom flanges. Due to the horizontal curvature, radial forces develop on the flanges to establish equilibrium. The lateral load on the flange, F_r, varies along its length and in proportion to the bending moment as required for radial equilibrium :

$$F_r = \frac{M}{hR} \tag{2.21}$$

where M is the total bending moment on the girder at that location, h is the distance between flanges, and R is the radius of the girder. The distribution of these lateral flange loads is shown in Fig. 2.7. The diaphragms restrain lateral bending of the girders, acting as lateral supports for the flanges. In the approximation, the diaphragms are assumed to be rigid supports against lateral bending.

The moments resulting from this loading would be the flange warping moments, M_f. The flange moments vary along the length of the flange. The warping normal stress is then given by :

$$\sigma_w = \frac{M_f}{S_f} \tag{2.22}$$

where S_f is the section modulus of the bottom flange. The longitudinal bending stress and warping stress distributions on a girder cross section are shown in Fig. 2.8. The summation of the stress due to bending, σ_b, and that due to warping, σ_w, gives the total stress in the bottom flange, σ_t.

CHAPTER 3

ANALYSIS PROCEDURE

3.1 Introduction

There are two separate problems which are relevant to the analysis of curved bridge units. The first involves computing the moments, shears, longitudinal and warping stresses, and reactions which develop due to dead load and known positions of live loads. A direct analysis of the structure with the prescribed loads can be performed to compute the responses. The second problem involves computing the envelope values of maximum and minimum moments and shears that can occur on the bridge due to moving live loads. Because of the complicated geometry of curved girder units, it is not possible a priori to determine the load positions producing maximum response, so a series of analyses is required, one for each load position.

The approximate analysis procedure, based on the V-load method, presented in this chapter computes the response of multi-girder bridge units with variable radius of curvature with skew supports. The girders may be nonprismatic and include composite behavior of the steel girders and concrete slab. The loads acting on the bridge include the dead load and moving truck or lane loads. Live loads are applied on the bridge unit, acting on the composite section, after the girders and deck are constructed.

For horizontally curved bridges the analysis procedure uses equivalent straight girders with the V-load method described in Chapter 2. Two analyses of the equivalent straight girders are performed for each load case. The applied loads on the girder are called P-loads, and analysis of the girders subjected to these loads results in P-load responses such as M_p, V_p, R_p, the bending moments, shears, and reactions, respectively. Because of the horizontal curvature of the unit, V-loads act on the girders. The girders are analyzed a second time with the V-loads applied at the diaphragm locations. The response due to these V-loads result in V-Load responses M_v, V_v, R_v, the bending moments, shears, and reactions, respectively. For a single load case then, the response of the horizontally curved unit is the sum of the P-load and V-load responses.

The matrix stiffness method is used to calculate the response of a girder to individual load cases. Each nonprismatic girder in the unit is modeled by an arbitrary number of prismatic beam elements, with constant properties for each element, connected at nodes. The individual elements can have different section properties, noncomposite, composite, or transformed for different load cases. The structural stiffness matrix is assembled from the element stiffness matrices. For a single load case, this structural stiffness matrix is factored and back-substituted with the load vector to determine

displacements at the nodal points. Using these displacements the moments, shears, reactions, and stresses are computed in the beam elements.

The matrix stiffness method can be used efficiently in generating envelopes of minimum and maximum responses. In the problem with moving live loads the position of the loads change but the structural stiffness matrix does not; it is independent of the loads. The stiffness matrix can be assembled and factored once and used to obtain responses for the different load positions. Influence functions are introduced and used in the envelope procedure as described in Sec. 3.3.

An important requirement of the analysis is to compute the response values along the entire length of the girders, not just at the nodes. The more locations at which the response is known the better the resolution of the maximum and minimum response. The locations along the girders at which responses are computed are called grid points. The analysis procedure automatically generates grid points along each girder using the geometrical properties of the bridge unit and a desired level of response resolution. In computing the envelope values these grid points are used to locate the moving load. Each concentrated live load is placed at each grid point to assure that the maximum moment is found at all the grid points.

3.2 Analysis Procedure for Single Load Case

3.2.1 Model of Bridge Unit. The geometrical layout of the bridge unit is described by a reference line from which the girders are related. The reference line is represented as segments of constant curvature, possibly with tangent sections. The radii of the reference line segments are computed from its arclength and the corresponding angle of curvature. Supports, which may be radial or skew, are located along the reference line. Each girder in the unit is located a constant radial distance from the reference line along the entire length of the bridge unit.

The analysis procedure allows nonprismatic girders. Each girder in the bridge is modeled independently by beam elements connected by nodes. A beam element is created wherever there is a change in section properties of the girder. Additional nodes are required at each support even if the section properties of the girder do not change. Radial diaphragms between the girders are located arbitrarily along the length of the unit.

The grid points are the locations at which the response quantities are calculated and are used to position the moving load. The support locations (including skew) and diaphragm locations are used to generate the grid points along the

girders. It is possible to establish additional grid points to increase the resolution of the responses.

3.2.2 Analysis of Girders for Single Load Case. The curved girders are separated, straightened and each modeled by prismatic beam elements. The response of the girders is computed using the matrix stiffness method by solution of the equilibrium equations:

$$K*U = P$$

for each girder, where K is the structural stiffness matrix assembled from beam element stiffness matrices, P is the load vector for the load case, and U are the resulting displacements. Displacements are computed for each degree of freedom of the girder. Each node has two degrees of freedom, a vertical translation and rotation. Vertical degrees of freedom at the support locations are deleted.

Because of the modelling of the girders by beam elements the stiffness matrix is banded, with a semi-bandwidth of four. A banded storage and equation solution procedure is used to minimize memory requirements and computation time in the equation solution procedure.

The nodal displacements of the girders are used to compute the internal forces at the ends of the elements. The internal forces at all the grid points of the girders are computed accounting for concentrated or distributed loads on the

elements. The reactions at the supports are computed from the shears on each side of a support.

3.2.3 Analysis of Bridge Unit For Single Load Case. The analysis of a bridge unit uses the procedure described in Sec. 3.2.2 for the response of each girder. The first load case is that of the P-loads which are applied to the unit; the resulting responses are denoted P-load responses. The moments, M_p, in the girders are summed at each diaphragm location and the V-loads are given by Eq. 2.19. These V-loads are applied to each girder at the diaphragm locations as a second load case. The response analysis of Sec. 3.2.2 is again performed for each girder using the V-loads, and the responses computed are denoted as V-load responses. The total response of the horizontally curved bridge unit is then the sum of the P-load and V-load responses for each girder :

$$M_t = M_p + M_v$$

$$V_t = V_p + V_v$$

$$R_t = R_p + R_v$$

The analysis of a bridge unit for a single load case can be summarized as :

1. Determine P-loads
2. Perform single load case analysis of girders with P-loads for P-load responses

3. Compute V-loads
   3.1 Sum moments at the diaphragms
   3.2 Compute V-loads at each diaphragm

4. Perform single load case analysis of girders with V-loads for V-load responses

5. Add the P-load and V-load responses for the total responses of the girders

3.3 Computation of Response Envelopes

The determination of the maximum and minimum response due to moving wheel loads requires analyses of the unit for numerous positions of the loads. Because each load case requires two analyses, P-load and V-load, for every girder, the number of solutions is very large. To improve the efficiency of the analysis for moving loads, influence functions for the girders are used to compute envelopes. Influence functions are responses in the beam elements due to a unit load at each degree of freedom. The influence functions are computed by placing a unit load on each degree of freedom and solving for the moments and shears in each beam element, and reactions at the supports.

To use the influence functions for the computation of response envelopes, the position of the wheel loads on the unit is first determined. Once the load vector P is calculated for each wheel load position, it is multiplied directly by the influence functions to obtain the moments, shears, and the reactions for each girder due to the P-loads. The V-load

responses are computed by multiplying the V-loads by the same influence functions for the girders. The responses are then computed at all grid points of the girders and the minimum and maximum values are saved. The loading is placed so that each concentrated load in the load pattern is placed on each grid point to guarantee maximum moment at that grid point.

The procedure to compute the response envelopes can be summarized as :

1. Determine the influence functions
   - 1.1 Assemble the banded structural stiffness matrix from the element stiffnesses
   - 1.2 Factor the stiffness matrix
   - 1.3 For each of two degrees of freedom per node :
     - 1.3.1 Apply a unit force at the node
     - 1.3.2 Back substitute for displacements
     - 1.3.3 Calculate member end forces
     - 1.3.4 Form influence functions for moment, shears, and reactions
2. Determine the position of the moving load along the reference line so that each load acts at each grid point
3. Multiply the load vector by the influence functions to obtain the moments, shears, and reactions due to the P-loads for each girder
4. Compute the V-loads
5. Multiply the V-loads by the influence functions to obtain V-load moments, shears, and reactions for each girder
6. Sum P-load and V-load response for the total response
7. Determine minimum/maximum response quantities at grid points

8. Repeat steps 2 thru 7 until moving load is no longer on the bridge unit

3.4 Computation of Flange Warping Stresses

As described in Chapter 2, the flanges of the girders are subjected to warping due to torsion induced by the horizontal curvature of the bridge unit. In composite girders the concrete slab acts together with the top flange to resist the warping moment. The section modulus for lateral bending of the top flange and slab is much larger than for the bottom flange resulting in smaller warping stresses. Generally only the warping of the bottom flange is important in composite systems.

In the approximate analysis procedure, the bottom flanges of the girders are straightened and modeled as individual flange elements supported at each diaphragm location. The curvature of the flanges is the same as that of the girders. Support locations, coordinates, and grid points are generated for the flanges as described in Sec. 3.2.1.

Using the model of the bottom flanges an analysis of the lateral bending can be performed after the loads are specified. As described in Chapter 2, the lateral bending of the flanges is caused by the radial flange forces which develop due to the horizontal curvature. The forces which act on the flange are computed using Eq. 2.21 in Chapter 2 and vary along the bridge in proportion to the total bending moment in the girders. To

compute lateral bending stresses in the flange, the lateral force on the flange is applied to the flange model using equivalent concentrated loads at the grid points of the original girder. The distributed lateral load at a point is considered to be an average value between adjacent points. These loads are used to compute the bottom flange warping moments, M_f, by the same single load case analysis procedure for the girders. Because the moment used to determine the lateral forces on the flanges is the sum of M_v and M_p for each girder, a separate V-load analysis of the flange is not required.

The flange warping moments act about the strong axis of the flange. The stress at the tip of the flange is given by $\sigma_w = M_f / S_f$ where S_f, is the section modulus of the flange. The sign of the stress as in tension or compression depends on the sign of the moment and which tip of the flange is under consideration. Figure 2.8 shows the distribution of warping stresses and bending stresses on a girder. The maximum total stress in the flange is then the combination of the warping stress and the longitudinal bending stress which gives the largest value.

CHAPTER 4

RESPONSE OF CURVED GIRDER BRIDGE UNITS

4.1 Introduction

This chapter presents the response of several idealized bridge units and compares the results of the approximate V-load analysis with the results from a finite element analysis procedure developed for horizontally curved bridges (7). To evaluate the accuracy of the V-load analysis and the important parameters on the response of bridge units, several bridge schemes are analyzed. A single span two girder curved bridge unit is analyzed in the first set of comparisons. In the second set of comparisons, a three span, four girder bridge unit is analyzed. For this second set of comparisons the radii of curvature, diaphragm spacing, and the support orientation are varied.

In the finite element analysis, the bridge unit is divided into three-dimensional substructures modeled by one- and two-dimensional finite elements. Reference 7 gives details of the finite element analysis for curved bridge units. Diaphragms are modeled as beam elements connected to the top and bottom flanges of the girders. The concrete slab is modeled as two dimensional plate elements connected to the girders by rigid beam elements. The properties of the plate elements may be different in the

transverse and longitudinal directions. When the concrete is considered ineffective, as in the negative moment regions, the slab can still transmit forces transversely to the girders. In this case, the elastic modulus in the longitudinal direction is small, but the modulus in the transverse direction is unaffected by the negative moments. In the finite element method the loads are represented by equivalent concentrated forces placed at the nodes of the mesh.

For the purpose of evaluating the approximate V-load analysis the bridge models used in the V-load and finite element analyses were matched as much as possible. The curvature and span lengths of each bridge model are identical, as are the locations of the radial diaphragms. The girder section properties were modified in the V-load analysis to correspond to the model used in the finite element analysis. The dead load used in the V-load analysis was computed from the tributary slab weight and the girder weight.

A major difference in the two models is the representation of composite behavior of the bridge unit. In the finite element analysis the torsional stiffness of the slab is represented by the plate elements. The torsional stiffness of the slab is not accounted for in the V-load analysis, although composite behavior in the longitudinal direction is recognized. The effect of the difference in modeling the torsional behavior

of the curved bridge unit will be apparent in the comparisons of the V-load and finite element response results.

4.2 Two Girder, Simple Span Bridge Unit

To evaluate the accuracy of the V-load method, a two girder bridge unit with simple spans is analyzed. Comparisons of the longitudinal bending stresses, warping, and total stresses are made for dead load, live load, and combined dead and live load for four variations of important parameters.

A plan view of the bridge is shown in Fig. 4.1a, cross section A-A of the bridge unit is shown in Fig. 4.1b. The table in Fig. 4.1 lists the parameters R, θ, and d defining Schemes A, B, C, and D that are studied in this section. The reference line, RL, is at the centerline of the bridge, and the arclength along this reference line is 100 feet. The diaphragms and end supports are radial. The centerlines of the girders are spaced at 6 feet. The concrete deck slab is 7-1/2 inches thick and the modular ratio of the concrete is eight. The noncomposite and composite moments of inertia for each girder are 12,626 in^4 and 35,874 in^4, respectively.

The girders were designed for noncomposite action under dead loads and composite action under live loads. The dead load consists of the weight of the steel girders, 0.111 k/ft, and the concrete deck slab, 0.563 k/ft. The live load is a standard

AASHTO HS20-44 truck (1), placed as shown in Fig. 4.2, with the spacing between the axles set at 14 feet. The wheels of the truck are placed directly on each girder so no transverse distribution factors are used. This is done to facilitate direct comparison of the V-load and finite element response results.

The placement of the truck shown in Fig. 4.2 produces maximum moments and bending stresses in the girders. This location was found using the V-load envelope procedure described in Chapter 3. The location of wheel loads to produce maximum moments for the four schemes is approximately the same, so the location of wheel loads shown in Fig. 4.2 is used for each scheme.

4.2.1 Response Comparisons. The response obtained from the V-load and finite element analyses are compared for dead load, live load, and combined dead and live load cases. The values listed are the stresses at midway through the bottom flange thickness at locations of approximately maximum bending stress, near midspan, unless otherwise noted. The percentage difference between the V-load and finite element results is calculated by :

$$\% D = \left(\frac{\text{V-Load} - \text{FEM}}{\text{FEM}}\right) * 100$$

Dead Load. The dead load stresses are computed by applying the dead load to the noncomposite steel girders. Comparison of the maximum longitudinal bending stresses for the four schemes is shown in Table 4.1a. The maximum stress in girder 1 is much larger than the stress in girder 2. The V-load maximum stress for girder 1 is computed to be within 4.1% of the finite element stress. All V-load stresses for girder 1 are conservative. For girder 2 the V-load stresses are less than those of the finite element values by as much as 10.6%. The largest percent difference in stresses for both girders occurs in Scheme D which has the sharpest curvature. The magnitude of stress is not sensitive to the diaphragm spacing. Figure 4.3 shows the longitudinal bending stress on the girders due to dead load for Schemes B and D (10 ft diaphragm spacing). The results clearly demonstrate the shifting of load from inner to outer girder which occurs in a horizontally curved bridge unit. Both the magnitude of the stress and the difference between the V-load and finite element values increases with a decreasing radius of curvature.

Figure 4.4 shows the warping stresses due to dead load for the 500 ft radius units. Peak warping stresses occur at the diaphragm locations and decrease with decreasing diaphragm spacing. The V-load warping stresses are larger than the corresponding finite element warping stresses at these diaphragm

locations and less than the finite element values at points between diaphragms. In the V-load method large warping stress exists at diaphragm locations because the diaphragms are assumed to restrain warping without lateral deflection. The diaphragms are assumed to be infinitely stiff and provide rigid supports for the flange. This assumption is not made in the finite element method.

As described in Chapter 2, the warping stress combined with the longitudinal bending stress gives the total stress at the tip of the bottom flange. Comparison of the warping plus bending stresses due to dead load is made in Table 4.2a. The stresses are compared between the diaphragms near the point of maximum bending stress at the locations listed. This is done because of the difference in modelling the flanges by the two analysis methods for the computation of the warping stresses.

Warping plus bending V-load stresses are between 8.4% and 49.5% underestimated when compared to the finite element values. The V-load stresses of girder 1 are closer to the finite element values than the stresses of girder 2. The percent differences are larger than those computed for the longitudinal bending stresses in Table 4.1a.

Figure 4.5 shows the dead load longitudinal bending plus warping stress curves for the 500 ft radius units. Peak stresses

again occur for the V-load values at diaphragm locations and the stresses for the 20 ft diaphragm spacing are larger than for the 10 ft spacing. The V-load stresses are generally lower than the finite element stresses for the 20 ft spacing but are only lower between diaphragms for the 10 ft spacing.

In summary, the V-load analysis underestimates the torsional stiffness of the unit for the transfer of loads between girders. This is evident by the conservative stress values for girders 1 and the unconservative values for girder 2 computed in the V-load analysis.

Live Load. The maximum longitudinal bending stresses due to live load on the composite section are listed in Table 4.1b. The trends in the live load response are similar to the dead load response: bending stresses are not dependent on the diaphragm spacing and the error in the V-load analysis increases as the radius of curvature decreases. The percent difference between finite element and V-load stresses is larger than for the dead load comparison because the torsional stiffness of the slab is important in distributing the live loads to the girders. Because the V-load analysis does not recognize the torsional stiffness of the slab, the stresses computed in the V-load analysis are much different than the finite element stresses. Again the V-load stresses for girder 1 are conservative while those for girder 2 are underestimated.

Table 4.2b lists the combined warping and longitudinal bending stresses from the V-load and finite element analyses due to live load. The addition of the warping stresses has little effect on the difference in live load stresses.

Dead Plus Live Load. The maximum longitudinal bending stress in the bottom flange due to dead plus live load is shown in Table 4.1c. Similar trends exist as in previous bending stress comparisons. The computed stress varies with the radius of curvature not with the diaphragm spacing. The percent difference for the combined load lies between that of the dead load and live load cases.

Figure 4.6 shows the bending stress in the girders for the combined dead and live load case for a 10 ft diaphragm spacing. This figure is similar to Fig. 4.3 but has higher stresses and a larger difference between the finite element and the V-load responses. The 500 ft radius shows a larger difference in stresses. The warping stresses for dead plus live load are shown in Fig. 4.7. The curves are similar to those in Fig. 4.4 but the magnitude of the warping stresses are larger. Peak V-load warping stresses occur at diaphragm locations.

Combining the warping stresses in the flange with the longitudinal bending stresses results in the total stress values for dead load plus live load as shown in Table 4.2c. The

difference for girder 1 is again much lower than for girder 2 and increases with the decreasing radius of curvature. Combining dead and live load partially compensates for the poor correlation of values for the live load case for girder 1, but there is little change in the difference for girder 2. Figure 4.8 illustrates the combined warping and bending stresses for the combined load case. The same trend in values exists as previously noted for the combined warping and bending stress dead load case.

Reactions. The reactions due to dead load for Schemes A & C are listed in Table 4.3. The shifting of load from inner to outer girder is seen here. The difference between V-load and finite element reactions is fairly small. The error in the V-loads magnifies the difference in moments but not reactions. Summation of the V-loads gives more accurate reactions than multiplication of the V-loads by the moment arm to obtain the bending moments.

4.2.2 Summary. The responses for the two girder horizontally curved bridge show some very definite trends. The spacing of diaphragms has no effect on the longitudinal bending stresses but does affect the warping stresses. As the radius of curvature decreases the stress in the outer girder increases. The shifting of load from inner to outer girder is present but it appears that the V-load procedure overestimates the transfer of load. The slab contributes torsional stiffness to the unit which

is not accounted for in the V-load analysis for live load. Because the largest difference of the two response results in the live load case, the torsional stiffness of the slab appears to have more effect on the distribution of load between the girders.

In the approximate analysis, the V-loads are applied at diaphragm locations, but the diaphragms do not contribute to the torsional stiffness of the bridge unit. The finite element analysis recognizes the contribution of the diaphragms to the torsional stiffness of the bridge unit. Because the transfer of forces between girders is related to the torsional stiffness of the bridge unit, the less the torsional stiffness of the bridge unit the greater will be the shift of forces from the inner to the outer girders.

4.3 Three Span, Continuous Bridge Unit

This section presents the response results of a typical curved girder bridge unit to investigate the response characteristics and the accuracy of the approximate V-load method. The longitudinal bending and warping stresses due to several load cases will be compared for different bridge configurations. The parameters considered in the bridge configurations are the diaphragm spacing, the radius of curvature, and the support orientation.

A plan of the horizontally curved bridge unit is shown in Fig. 4.9. The bridge is three continuous spans with a total length of approximately 272 feet, constant radius of curvature, R, of 175 feet along the reference line, and radial supports. The girders are spaced at 7ft 4in. and identified R_1, R_2, R_3, and R_4, from outside to inside. The diaphragms are spaced at a distance, d, of 10.46 feet along the reference line. The concrete deck slab is 8 inches thick and the modular ratio for the concrete is eight. On each side of the bridge, the slab overhangs 3-ft 8-in.

The four, nonprismatic girders have the same cross section as shown in Fig. 4.10. The girders were designed for noncomposite action under dead load. The noncomposite moment of inertia in negative and positive bending regions is 36,348 in^4 and 18,570 in^4, respectively. Under live load, composite action is assumed in positive moment regions and noncomposite action in negative moment regions. The composite moment of inertia in the positive moment region is 45,678 in^4.

To study the response of curved bridge units, variations of this standard bridge will be examined. The bridge configurations studied are :

Bridge 1 - Standard Bridge with diaphragm spacing of 10.46 feet, radius of curvature of 175 feet, and radial supports

Bridge 2 - Bridge 1 with the diaphragm spacing changed from 10.46 feet to 20.92 feet

Bridge 3 - Bridge 1 with the radius of curvature changed from 175 feet to 350 feet

Bridge 4 - Bridge 1 with the two interior supports skewed as shown in Fig. 4.11

The dead load consists of the weight of the steel girders and the concrete deck slab. The concrete deck slab weighs 0.733 k/ft and the steel girders 0.317 k/ft over the supports and 0.179 k/ft elsewhere. The live load is a single AASHTO HS20-44 truck (1). Lane loads were not considered for this study. The longitudinal placement of the truck on the unit to produce maximum stresses in girder 1 was determined using the V-load envelope procedure described in Chapter 3. The truck was placed at two different transverse locations on the bridge deck, an outer position and a middle position. Figure 4.12 shows the location of the wheel loads on the bridge for each placement. The wheel loads were placed directly on the girders to minimize distribution effects of the deck slab. The finite element solution does not need distribution factors. Lateral distribution factors are therefore not included in this analysis in order not to complicate evaluation of the V-load analysis.

4.3.1 Response Comparisons.

Effect of Curvature. Bridges 1 and 3 are compared to determine the importance on the responses of a curved bridge unit of the radius of curvature. The reference line radii in Bridge 1 and 3 are 175 feet and 350 feet, respectively.

Dead Load. The longitudinal bending stresses due to dead load for Bridges 1 and 3 are listed in Table 4.4a. The stresses are given for two locations along the four girders, near the point of maximum bending stress. There is a large shift of load from girder 4 to girder 1 in Bridge 1, with the shift less for the larger radius of curvature in Bridge 3.

The percent difference between finite element and V-load stresses, computed as for the simple span case, is also listed in Table 4.4a. The largest difference for any of the bending stresses of Bridges 1 & 3 is 14.7%. Negative stresses are not predicted by the V-load method as accurately as positive stresses. All V-load results are on the conservative side for Bridges 1 and 3. This contrasts with the results for the simple span bridge unit (see Table 4.1a).

Figures 4.13 and 4.14 show the dead load bending stresses in girders 1 and 4 of Bridges 1 and 3; The comparison between the stresses computed using the V-load method and finite element method is very good. The girder 1 stresses in Bridge 1, with the smaller radius of curvature, are larger than those for

Bridge 3. The opposite is true for girder 4. As the radius of curvature increases the difference between V-load and finite element stresses decreases.

The warping stresses in the bottom flange due to dead load for girders 1 and 4 of Bridges 1 and 3 are listed in Table 4.5a. The warping stresses are given at two locations near the maximum bending stress, but not at a diaphragm location, because of the difference in modeling of the flanges in the two methods. The percent difference between the V-load and finite element warping stresses are very large in the two bridges, although the largest warping stress is only 1.57 ksi for Bridges 1 and 3.

The warping plus bending dead load stresses for girders 1 and 4 are listed in Table 4.6a for certain locations. For Bridges 1 and 3 the difference in V-load and finite element responses are within 10.5% and are much less than the warping stress differences found in Table 4.5a. The V-load stresses are slightly smaller than the finite element stresses.

Figures 4.15 and 4.16 illustrate the V-load and finite element dead load stresses due to bending and warping for girders 1 and 4 of Bridges 1 and 3. Again the results of the approximate method are very good. The stresses have increased with the addition of the warping stresses, which can be seen by comparing Figs. 4.15 and 4.16 with Figs. 4.13 and 4.14. The V-load method

predicts higher warping stresses at diaphragms than found from the finite element method. This V-load peaking of stresses at diaphragm locations is due to the assumption that the flange is rigidly supported at the diaphragms. The peaks are more noticeable in Bridge 1 with the smaller radius of curvature and also more noticeable in the positive bending regions of the girders. Between diaphragms the finite element warping stresses are larger or very close to those of the V-load analysis.

Live Load. An AASHTO HS20-44 truck was placed on the bridge at two transverse locations. In the outer load position, the wheel loads are placed directly on girders 1 and 2. In the middle load position, the wheel loads are placed directly on girders 2 and 3.

Tables 4.4b and 4.4c list the longitudinal bending stresses for girders 1 and 4 due to the two live load placements on Bridges 1 and 3. The V-load stresses are conservative for girder 1 when the live load is placed in the outer position.

The bending stresses in Bridges 1 and 3 for the middle load placement show poor correlation between analysis methods. For girder 1 the V-load stresses are as much as 80.5% less than the finite element stresses. The percent difference for girder 4 is even worse.

Figure 4.17 illustrates the V-load and finite element stresses for girders 1 and 4 for the two live load placements on

Bridge 1. The V-load and finite element curves in Fig. 4.17a and 4.17b for the outer load position are more similar than those in Figs. 4.17c and 4.17d for the middle load position. For the first span of girder 4 for the middle load position, Fig. 4.17d shows a difference in sign between the V-load and finite element values in the bending stress.

The difference in response predicted by the two methods results from the transverse distribution of loads to the girders by the slab. The V-load method does not account for distribution of the load by the slab.

The outer live load position induces torque on the bridge unit. Since the V-load method does not include transverse distribution, but does overestimate the torque due to curvature the V-load stresses for this position are close to the finite element stresses. But since the middle load position does not induce additional torque on the bridge unit, the V-load stresses are worse due to the V-load methods overestimation of the torque. The slab participation should be basically the same for the two live load positions.

The warping stresses in girders 1 and 4 due to live load are listed in Tables 4.5b and 4.5c. The maximum warping stress for the outer load position for girder 1 is approximately 1.65 ksi by the finite element analysis and 1.04 ksi by the V-load

analysis for the outer load position. For the inner load position the maximum stress is again for girder 1 and is 0.83 ksi from the finite element analysis and 0.21 from the V-load analysis. The correlation of warping stresses between methods is very poor; the minimum difference is 37%. The V-load warping stresses are unconservative. Because the live load bending stresses are in substantial error it can be expected that warping stresses will be in even more error because they are computed from the live load bending moments.

Table 4.6b and 4.6c list bending plus warping stresses in the bottom flange for both live load placements. For the outer load position the percent difference for girder 1 of Bridges 1 and 3 is a maximum of 5.9%, while that for girder 4 is larger. The stresses in girder 4 are underestimated by the V-load method. The V-load and finite element stresses for the middle load placement are very poor.

The live load bending and warping stresses computed in the finite element and V-load analyses are shown in Fig. 4.18 for girder 1 and 4 of Bridge 1. The outer live load position gives closer V-load and finite element responses for reasons discussed above.

Dead Plus Live Load. Figure 4.19 shows the bending plus warping stresses due to combined dead and live load on girders 1 and 4 of Bridge 1 for both load placements. For the combined load

the agreement between the V-load and finite element stress curves for girder 1 is good, regardless of the load placement. The magnitude of the stress for girder 1 is slightly larger for the outer load position as expected. The peak stresses at diaphragms are less noticeable in the V-load results of girder 4, (Figs. 4.19b and 4.19d). The V-load stresses are conservative for both girders of the outer load position but not for the middle position. Combining the dead and live load stresses reduces the difference between V-load and finite element results seen in the live load stresses of Figs. 4.17 and 4.18 because the large dead load stresses are accurately predicted by the V-load method.

Effect of Diaphragm Spacing. The effect of the diaphragm spacing on the stresses computed in a horizontally curved bridge unit can be seen by examination of Bridges 1 and 2. Bridge 1 has a diaphragm spacing of 10.46 feet and Bridge 2 a diaphragm spacing of 20.92 feet.

Dead Load. The longitudinal bending stresses in Bridges 1 and 2 due to dead load are given in Table 4.4a for all four girders. The V-load analysis overestimates both the positive and negative stresses in all the girders. The difference between the V-load and finite element values is a maximum of 14.9% for Bridge 2 and 14.2% for Bridge 1. The positive and negative bending

stresses, computed in both analyses, are not affected by the diaphragm spacing, as seen with the simple span case of Sec. 4.2.

The warping stresses in the bottom flange due to dead load are listed in Table 4.5a for girders 1 and 4. The magnitude of the warping stresses between the diaphragms increases with increasing diaphragm spacing. Also, as the diaphragm spacing increases, the difference between V-load and finite element warping stresses between the diaphragms decreases.

Table 4.6a lists the warping plus bending dead load stresses in girders 1 and 4. As the diaphragm spacing of Bridge 1 is increased to 20.92 feet the total stress computed by the V-load method increases slightly for girder 1 and decreases slightly for girder 4. The percent difference between the V-load and finite element stresses increase in Bridge 2, mainly near the end support where the end conditions are different in the two analyses.

The bending plus warping stresses due to dead load for Bridge 2 are illustrated in Fig. 4.20 for girders 1 and 4. The peak stresses that occur at the diaphragm locations are noticeable. The warping stresses have more effect on the total stress values for Bridge 2 than for Bridge 1 because an increase in diaphragm spacing produces larger warping stresses with little change in the longitudinal bending stresses.

Live Load. Tables 4.4b and 4.4c list the longitudinal bending stresses in girders 1 and 4 due to the outer and middle live load positions. As in the dead load bending comparison, the change in diaphragm spacing has little effect on the magnitude of the bending stress.

The warping stresses developed due to the live load, listed in Tables 4.5b and 4.5c, are affected by the diaphragm spacing. However, the difference between the V-load and finite element values are only slightly different in Bridge 1 than in Bridge 2. While the warping plus bending stresses computed by the V-load change little with the change in diaphragm spacing, the difference between V-load and finite element stresses does change. For Bridge 2 the V-load stresses in girder 4 with the outer placement are now conservative. The correlation between the responses of the two methods is better for the outer live load position.

Dead Plus Live Load. The warping plus bending stresses for combined dead and live load for Bridge 2 are shown in Fig. 4.21. The V-load stresses for girder 1 are much larger for the outer load position than the middle load position but those for girder 4 do not vary much with the live load placement. Comparing Fig. 4.21 to Fig. 4.19, which shows the warping plus bending stresses due to dead plus live load for Bridge 1, the effects of the diaphragm spacing are noticeable in the pronounced

stress peaks in Bridge 2. These peaks develop because of the larger warping stresses produced by the larger diaphragm spacing, and the V-load assumption that diaphragms rigidly restrain lateral bending of the bottom flange.

Effect of Support Orientation. The effect of the orientation of the supports is investigated by comparing the results from the V-load and finite element analyses for Bridges 1 and 4. Bridge 1, as shown in Fig. 4.9 has four radial supports. The two interior supports of Bridge 4 seen in Fig. 4.11 are skewed, one at 30° and the other at -4° with respect to the radial line. The span lengths in Bridge 4 are slightly different in all four girders due to the location of the supports. The finite element model was changed at the first interior support in Bridge 4 by the removal of an adjacent diaphragm to allow for proper modeling of the bridge unit at that point.

Dead Load. Table 4.4a lists the longitudinal bending stresses due to dead load for the four girders. The positive stress in the first span of girder 1 has increased with the introduction of the skew resulting because of the longer span length. The positive bending stresses in girders 1 and 2 and the negative bending stresses in girders 3 and 4 are not predicted as well using the V-load method in Bridge 4 as in Bridge 1. Figure 4.22 shows the longitudinal bending stress due to dead load for

girders 1 and 4 of Bridge 4. Comparing this with Fig. 4.13, the differences between the V-load and finite element results are largest in girder 1 for Bridge 4 and in girder 4 for Bridge 1.

The warping stresses in girders 1 and 4 due to dead load are shown in Table 4.5a. For Bridge 4 the warping stresses show a different sign at 0.288L than occured at the same location in Bridge 1 because of the skewed support. The difference is about 60.4% for Bridge 4 compared to 36.5% for Bridge 1. Combining the warping and bending stresses results in the stresses shown in Table 4.6a for dead load. The total stress in the positive region of girder 1 has increased in Bridge 4 while that in the negative region has decreased. For girder 4 the effects are the opposite. The difference between the V-load and finite element stresses is larger for the bridge with the skewed supports than the bridge with the radial supports.

Figure 4.23 shows the bending plus warping stresses due to dead load for girder 1 and girder 4 of Bridge 4. The change in span lengths, which corresponds to a change in moments and stresses, can be seen by comparison of Fig. 4.23 and Fig. 4.15. The removal of the diaphragm around the first interior support is evident by the peak in the finite element stress at that location for girder 4 (Fig. 4.23b).

Live Load. The bending stresses for girders 1 and 4 due to live load for the outer and middle positions are listed in

Tables 4.4b and 4.4c. The skew affects the live load stresses near the interior supports of girder 1 for the outer live load placement. The percent difference between V-load and finite element responses also increases for this point. Because the diaphragm spacing is not altered in Bridge 4, except at the first interior support, the live load warping stresses are not affected except around that support.

As with the previous case, the outer live load placement results in better correlation between the V-load and the finite element results than does the middle live load position. The decrease in the difference for Bridge 1 when warping and bending live load stresses are combined also occurs for Bridge 4.

The skewed supports do not have much effect on the stresses computed other than due to the changes in span lengths.

Dead Plus Live Load. Figure 4.24 shows the warping and bending stresses in Bridge 4 due to combined dead and outer placement of live load. The results are very similar to those shown in Fig. 4.23 for warping plus bending stresses due to dead load for Bridge 4. The longer span lengths produce larger positive stresses in the first span of girder 1 for Bridge 4 compared to the stresses of Bridge 1 in Fig. 4.19. The stresses in girder 4 show a complicated variation near the interior support, because of the skew.

4.3.2 Summary. The responses for the four curved girder bridge units show the importance of certain parameters. As the radius of curvature increases, the shift of load from the inner girders to the outermost ones decreases. The diaphragm spacing does not affect the bending stresses, but it does affect the warping stresses. The larger the distance between diaphragms the larger the warping stresses at the diaphragm locations. Decreasing the diaphragm spacing decreases the magnitudes of the warping stresses and also decreases their influence on the warping plus bending stress values.

Skew supports affect the bending stresss responses because the span lengths are changed. As long as the diaphragm spacing does not change, the effect of skew supports on warping stresses is small.

The distribution of live load is particularly dependent on the distribution of load by the slab to the girders. The torsional stiffness of the slab is important in distributing the load. The V-load analysis makes no assumption on this torsional stiffness and does not include it in the approximate analysis.

CHAPTER 5

RESPONSE ENVELOPES FOR MULTIGIRDER BRIDGE UNITS

5.1 Introduction

In design, the minimum and maximum responses due to a truck load moving over the bridge are important. Envelopes for bending moment, shear force and reaction response, as computed by the procedures described in Chapter 3, are presented in this chapter for two bridge units.

To compute the live load responses, lateral distribution factors must be selected. The AASHTO straight girder live load lateral distribution factors are used to compute the live load, P-load, response of the girders (1). The AASHTO factors are defined as the fraction of truck wheel load carried by each girder and are based on attaining maximum moment in each girder (15).

To compute the V-loads needed for the V-load live load responses a seperate lateral distribution factor is required. Using the AASHTO live load lateral distribution factor for the V-load computation would result in too much load on the girders (15). The V-loads depend on the summation of moments at a section, not on the lateral placement of the load and are maximum when all lanes are loaded. Since the V-loads act concurrently on the girders for a given live load position the sum of the V-load

distribution factors acting at a section should equal the number of wheel loads acting in the section (15). Let NW be the number of wheel loads on a section, and NL the number of lanes loaded. Since the number of wheel loads per lane is two, NL is equal to NW / 2. A wheel load lateral distribution factor for NG girders is computed in Reference 15 as :

$$DF = 2 * NL / NG$$

On the inner girder, the P-load and V-load moments are usually opposite in sign. As shown in the comparisons of Chapter 4, the total response of the interior girder due to live load is usually less than obtained from a finite element analysis. To correct this deficiency, it may be desirable to decrease the V-load applied to the inner girder. Reference 16 suggests that for the inner girder, NL in the above equation equal the number of loaded lanes applied to the inner girder. To compute the DF for the remaining girders NL would be the number of lanes of the bridge which are loaded.

5.2 Envelope Computation

The envelopes of bending moment and shear force for Bridges 1 and 4 from Sec. 4.3 are presented here. The live load is one AASHTO HS20-44 truck with constant axle spacing of 14 feet. The AASHTO lateral wheel load distribution factors are 1.257 for the exterior girders, girders 1 and 4, and 1.333 for

the interior girders (1). These distribution factors are applied to the truck wheel loads, P-loads, at each position to compute the P-load responses.

The V-load distribution factor is computed using the expression given in the previous section. The number of lanes loaded is one and the number of girders is four resulting in a V-load distribution factor of 0.5 for all girders. To compute the V-loads on a specific girder due to the live load the live load moments are summed about the diaphragms as described in Chapter 3. Because these moments are computed using the factored AASHTO live loads the moments need to be multiplied by the ratio of the V-load distribution factor to the AASHTO factor. This multiplication adjusts the V-loads to have the distribution factor computed above. The ratio of the V-load distribution factor and AASHTO factor used in computing the live load V-loads are :

Girder 1 and 4 : .5 / 1.257 = .3978

Girder 2 and 3 : .5 / 1.333 = .3751

The truck moves along the bridge, placed at numerous points and the moment, shear, and reaction responses are computed. The minimum and maximum responses at each grid point are found by comparing responses due to each live load position.

Figures 5.1 through 5.4 show the minimum and maximum bending moments and shear forces for dead plus moving live load

for the girders of Bridge 1. The envelope curves have the same shape but because of the effect of the V-loads the magnitude of the response decreases from girder 1 to girder 4. Figures 5.5 through 5.8 show the envelopes for the girders of Bridge 4, which has skew supports. Because of the skew supports the girders are not symmetric about the bridge centerline. The length of the first span in girders 1, 2, and 3, is slightly longer due to the support line being rotated clockwise from the radial position.

Table 5.1 lists the bending moments and shear forces at three locations of the girders of Bridges 1 and 4. By introducing a skew of 30 degrees, span 1 of girder 1 increases by approximately 8.5 feet. As expected the moment at 0.13L of girder 1 increases, by 23%, while the moment at the first interior support decreases, by 2.1% compared to the corresponding values of Bridge 1. The location 0.13L is near midpoint of span one. For girder 4 the moment in span one decreases by 23.1% and the moment at the support increases by 5.4% due to the shortening of span one. The presence of a skew support has no other noticeable effect on the response envelopes.

Table 5.2 lists the minimum and maximum reactions resulting from a truck load moving across Bridges 1 and 4. For Bridge 1 the interior supports have the same minimum and maximum reactions. The interior support reactions for Bridge 4 are not

identical, reflecting the unsymmetric configuration of Bridge 4. The orientation of the supports in the two bridge configurations do not largely effect the reaction responses.

CHAPTER 6

SUMMARY AND CONCLUSIONS

6.1 Summary

An approximate analysis of horizontally curved bridge units has been presented using equivalent straight girder analysis. Each girder is straightened and modeled as individual beam elements with constant properties. The individual girders are then analyzed using the matrix stiffness method for the applied loads on the bridge, P-loads, which are dead or live loads.

The effects of the horizontal curvature of the unit are represented by a set of vertical shears, V-loads, acting on the girders at diaphragm locations. The V-loads are derived from the summation of P-load moments at the diaphragms and geometrical properties of the bridge as described in Chapter 2. The response of the girders is the sum of the P-load and V-load responses at locations along each girder. The responses computed are the bending moments, shear forces, reactions, and bending and warping stresses. This procedure is performed for each girder for every load case defined.

Envelopes of the girder response due to a moving truck load along the bridge are computed using influence functions. Influence functions are responses at each degree of freedom due

to a unit load at every degree of freedom, as described in Chapter 3. The influence functions are multiplied by the applied truck loads to obtain the responses of the girders to the truck load at a position. This procedure is efficient because it eliminates the repetitive solution of the equilibrium equations for truck loads at numerous positions along the bridge unit.

Warping moments also develop in the girders due to the horizontal curvature. The lateral bending of the flanges is assumed to be proportional to the longitudinal bending moment on the girder as detailed in Chapters 2 and 3. Loads are applied to the bottom flange of the girders which are straightened and modeled as individual beam elements with constant properties. The warping moments are converted to warping stresses using the section modulus of the flange. The warping stresses are combined with the longitudinal bending stresses to obtain the maximum stresses in the tip of the bottom flange.

The analysis techniques described were used to study the responses of two different bridge systems, a two girder simple span unit and a four girder, three span unit. To measure the accuracy of the approximate method the responses were compared with those from a finite element analysis of the identical bridge configurations. Correlation between the V-load approximate and the finite element responses were made for the different bridge configurations for both dead and live loadings. Envelopes of

minimum and maximum bending moment and shear force due to a truck load moving along the bridge were computed. The importance of certain bridge parameters; radius of curvature, diaphragm spacing, and support orientation, were also studied.

6.2 Conclusions

Shifting of load from the inner to outer girder is present in horizontally curved bridges. The bending stress due to dead load computed in the V-load analysis for the simple span unit was found to be conservative for girder 1 but unconservative for girder 2 when compared to finite element results. For the four girder, three span unit the V-load responses are conservative for all girders relative to finite element responses.

The difference between V-load and finite element responses are much greater for live load than for dead load. The torsional stiffness of the slab effects the distribution of live loads and the resulting live load stresses. The V-load method does not include the torsional stiffness of the slab but it is included in the finite element method. The responses obtained from the V-load analysis for live load are only as good as the lateral distribution factors assumed in the V-load method. When the responses due to dead plus live load are computed the correlation between V-load and finite element responses is better

than the live load only case but not as good as the dead load only case.

A decreasing radius of curvature of the bridge unit increases the longitudinal bending stress in the outer girder and decreases the bending stress in the innermost girder. The diaphragm spacing does not effect the longitudinal bending stress but does effect the warping stresses at the diaphragm locations. The larger the diaphragm spacing the larger are the warping stresses computed at the diaphragms. The presence of a skew support effects the bending moments and stresses by changing the span lengths of the girders. The error in the V-load method is greater for skew supports than radial supports, especially for live load.

REFERENCES

1. American Association of State Highway and Transportation Officials (AASHTO), Standard Specifications for Highway Bridges, AASHTO, Washington, D.C., Thirteenth Edition, 1983.

2. American Association of State Highway and Transportation Officials (AASHTO), Guide Specifications for Horizontally Curved Highway Bridges, AASHTO, Washington, D.C., 1980.

3. Culver, C., Brogan, D., and Bednar, D., " Analysis of Curved Girder Bridges," Engineering Journal, AISC, Vol. 7, No. 1, January 1970, p.10-15.

4. "Curved I-Girder Bridge Design Recommendations," Journal of the Structural Division, ASCE, Vol.10, No. 103, May 1977.

5. Gillespie, J.W., "Analysis of Horizontally Curved Bridges," Engineering Journal, AISC, Vol. 5, No. 4, October 1968, p.137-143.

6. Grubb, M.A., "Horizontally Curved I-Girder Bridge Analysis: V-Load Method," Transportation Research Record 982, p.26-36.

7. Hahn, K.H., Computer Program for the Analysis of Curved Girder Bridges, Thesis, Department of Civil Engineering, University of Texas at Austin, May 1987.

8. Heins, C.P., and Jin, J.O., "Live Load Distribution on Braced Curved I-Girders," Journal of the Stuctural Division, ASCE, Vol. 110, No. 3, March 1984, p.523-530.

9. Heins, C.P., and Siminou, J., "Preliminary Design of Curved Bridges," Engineering Journal, AISC, April 1970, p.50-61.

10. Heins, C.P., and Spates, K.R., " Behavior of Single Horizontally Curved Girder," Journal of the Structural Division, ASCE, Vol. 96, No. ST7, July 1970, p. 1511-1524.

11. Ketchek, K., " Another Approach to Simplified Design of a Curved Steel Girder, " Engineering Journal, AISC, Vol. 6, No. 4, October 1969, p.116-123.

12. McManus, P.F., and Nasir, G.A., "Horizontally Curved Girders-State of the Art," Journal of the Structural Division, ASCE, Vol.95, No. ST5, May 1969, p. 853 - 870.

13. Poellot, W.N., "Computer-aided Design of Horizontally Curved Girders by the V-load Method," Engineering Journal, AISC, First Quarter 1987.

14. Richardson, Gordon, & Associates, Consulting Engineers, "Analysis and Design of Horizontally Curved Steel Bridge Girders," United States Steel Structural Report, ADUSS 88-6003-01, 1963.

15. United States Steel Corporation "V-Load Analysis, " USS Highway Structures Design Handbook, ADUSS 88-8535-01, Vol. 1, Chapter 12, July 1984.

16. USS Engineers & Consultants, Inc., "VLoad User Manual," May 1985.

17. Weaver, W. and Gere, J.M., Matrix Analysis of Framed Structures, Van Nostrand Reinhold Company Inc., New York, 1980.

18. Weissman, H. A., "Straight-Element Grid Analysis of Horizontally Curved Beam Systems," Engineering Journal, AISC, April 1970, p.41-49.

VITA

Ann Louise Fiechtl was born in Quincy, Illinois, on June 19, 1960, the daughter of Arlene Pinkelman Fiechtl and Joseph Francis Fiechtl. After completing her work at Quincy Notre Dame High School, Quincy, Illinois, in 1978, she entered The University of Illinois in Champaign-Urbana, Illinois. She received the degree of Bachelor of Science in Civil Engineering from The University of Illinois in May, 1982. During the following years she was employed as a Civil/Structural Engineer for the Bechtel Power Corporation in Ann Arbor and Midland, Michigan. She also was employed as a Building Engineer for the General Telephone and Electronics Corporation in Bloomington, Illinois. In September, 1985, she entered the Graduate School of The University of Texas at Austin.

Permanent address: 1314 North 10th Street
Quincy, Illinois

This thesis was typed by Sharon Cunningham.

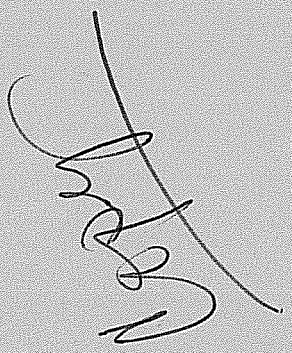

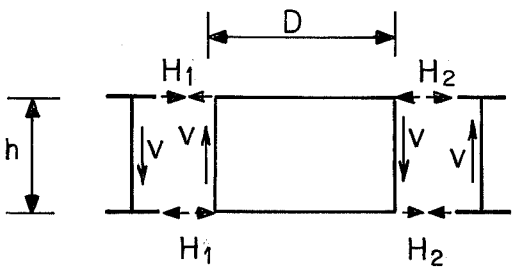
D
H1
H2
h
V
V
V
V
H1
H2

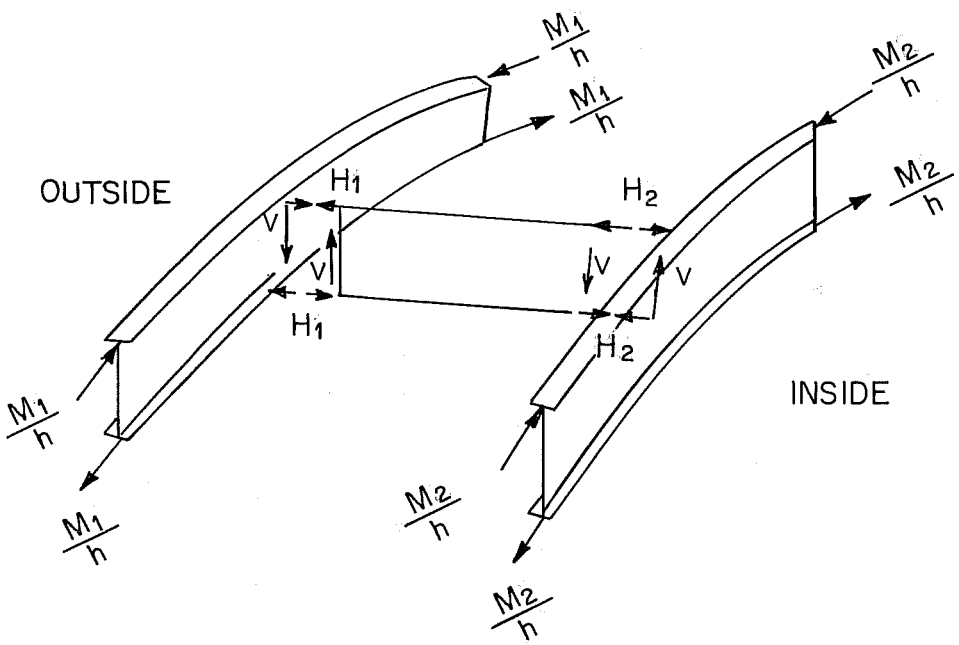
M1/h
M1/h
OUTSIDE
H1
H2
V
V
V
V
H1
H2
M2/h
M2/h
M1/h
M1/h
INSIDE
M2/h
M2/h

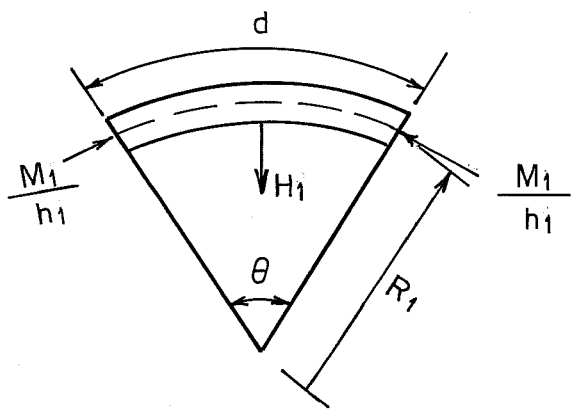
d
M1
h1
H1
θ
R1
M1
h1

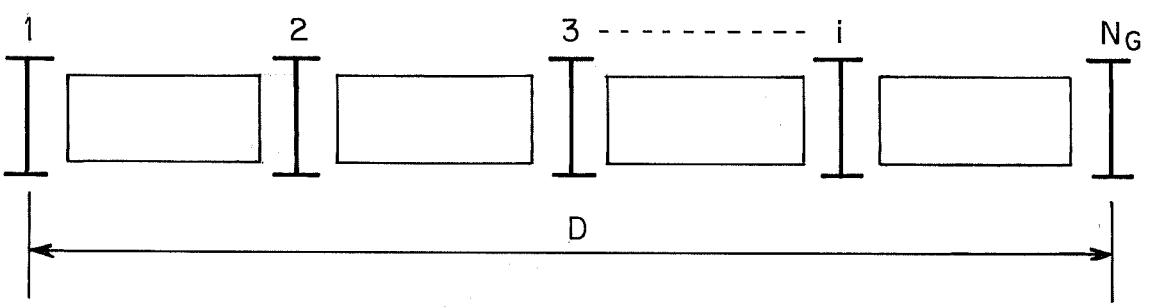
1
2
3
i
NG
D

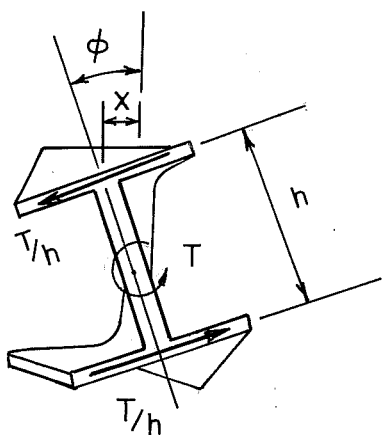
ϕ
x
h
T/h
T
T/h

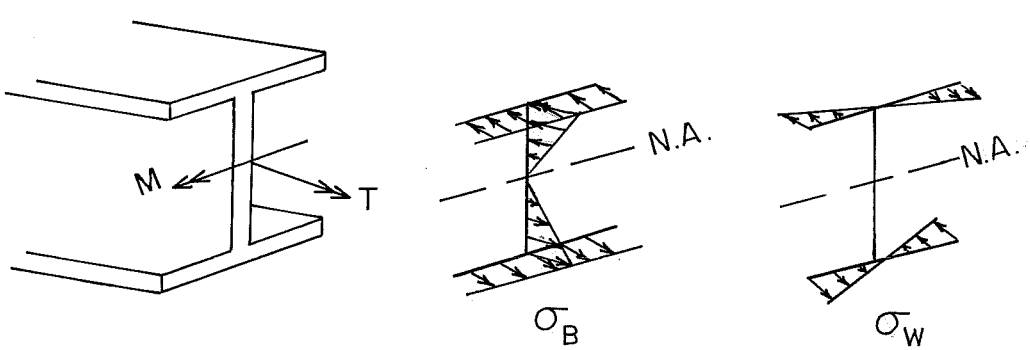
M
T
N.A.
N.A.
σB
σW

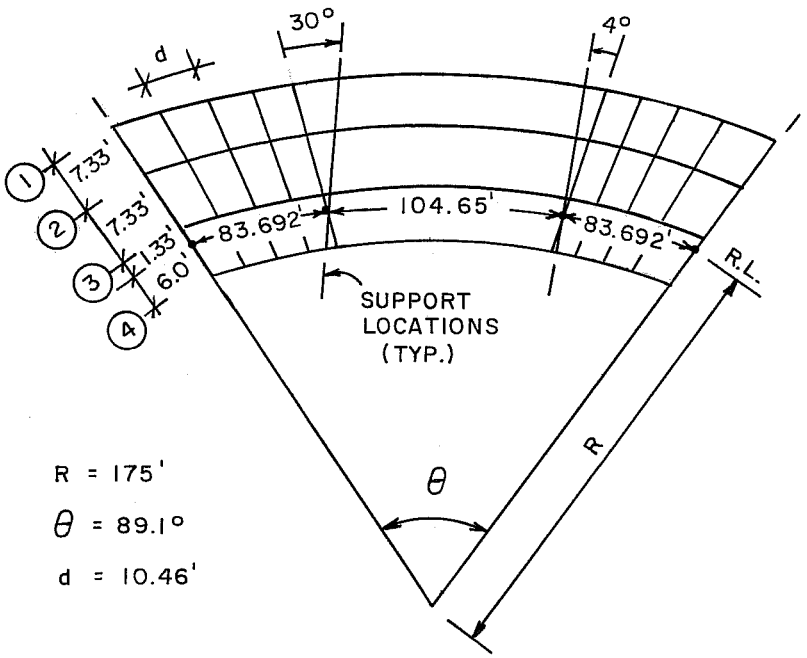

R = 175'

θ = 89.1°

d = 10.46'

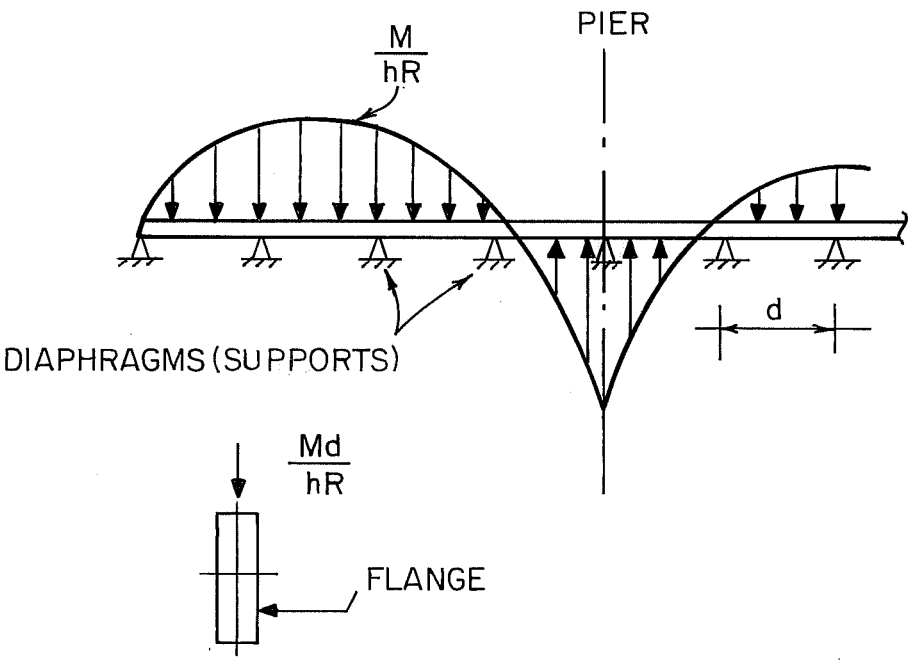
M
hR
PIER
d
DIAPHRAGMS (SUPPORTS)
Md
hR
FLANGE

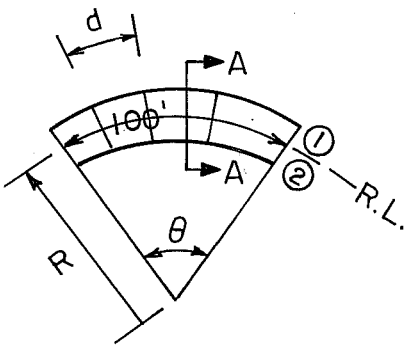

SCHEME	RADIUS R	ANGLE θ (°)	D.SPNG d
A	1000'	5.73	20'
B	1000'	5.73	10'
C	500'	11.46	20'
D	500'	11.46	10'

(a)

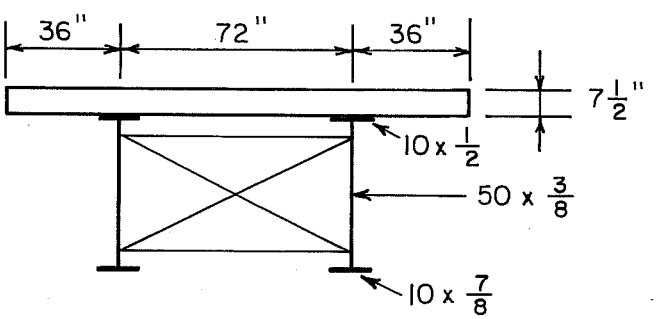

SECTION A-A

(b)

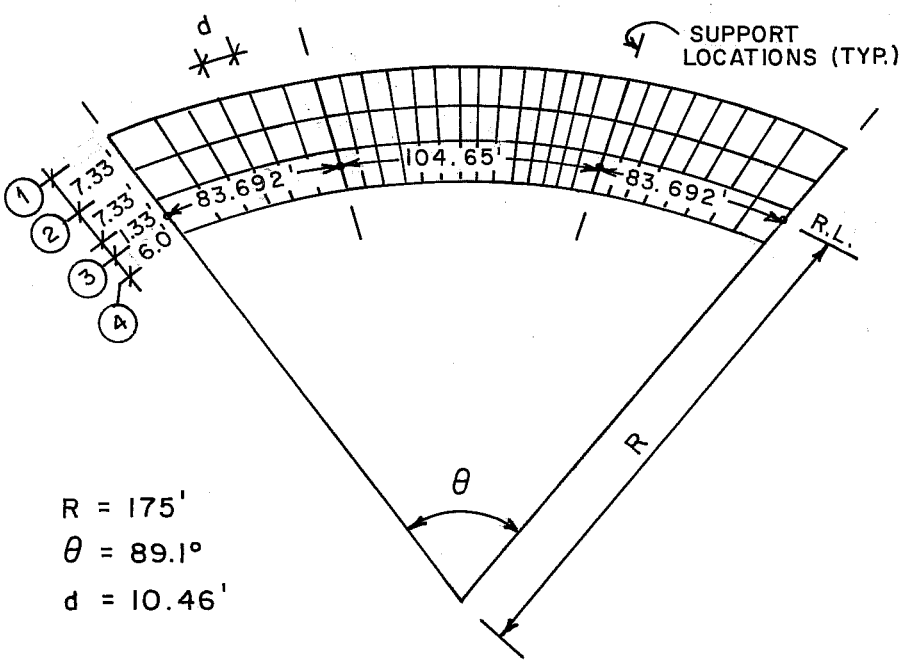

R = 175'

θ = 89.1°

d = 10.46'

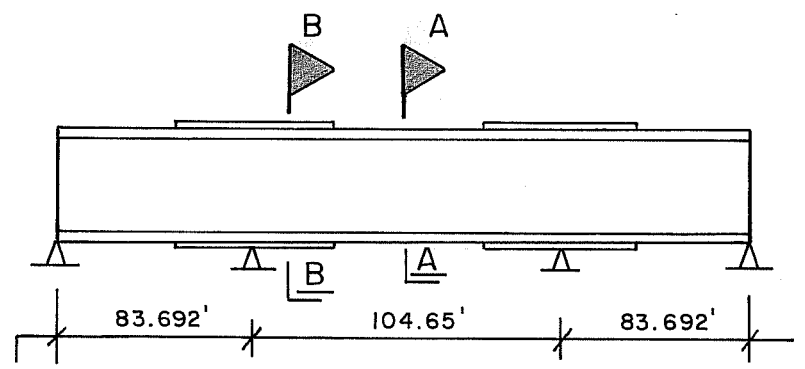

R.L. DIMENSION

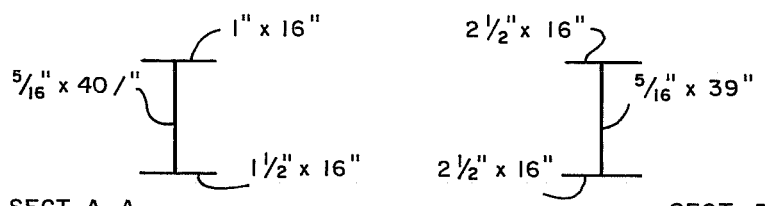

SECT. A-A

SECT. B-B

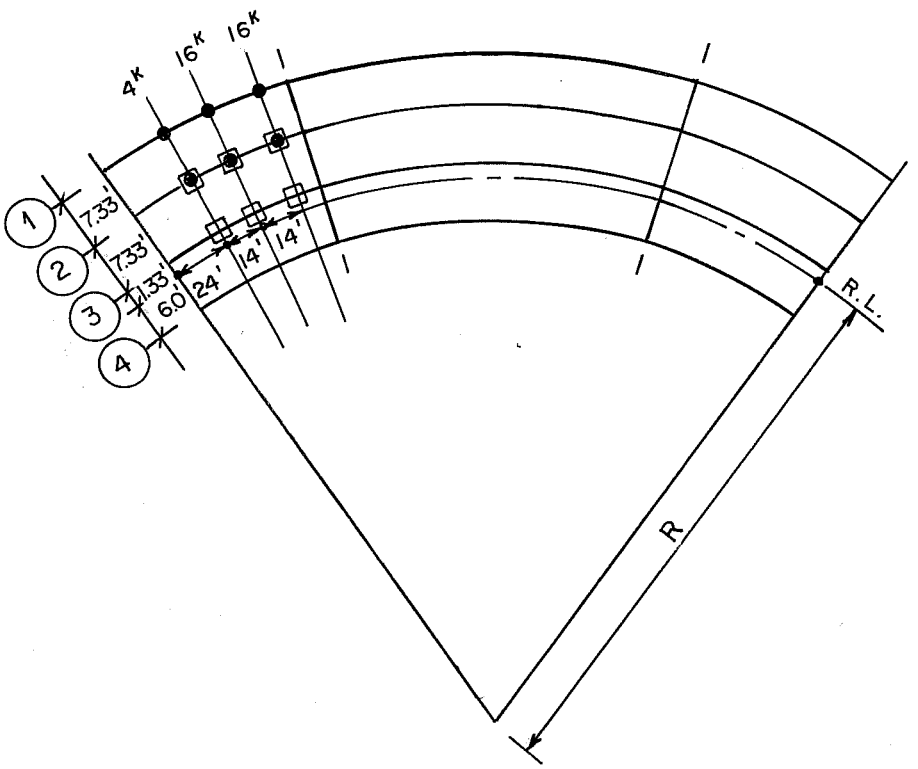

● OUTER LOAD POSTION

□ MIDDLE LOAD POSITION

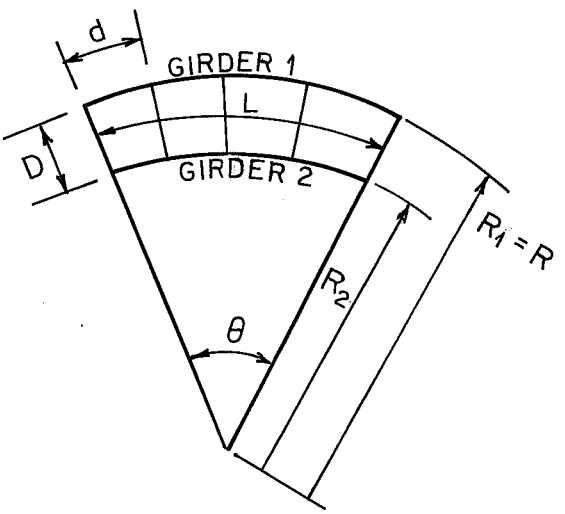
d
GIRDER 1
L
D
GIRDER 2
$R_1 = R$
R_2
θ

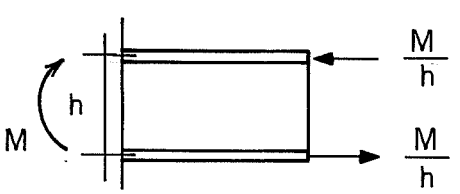
M
h
M
h
M
h

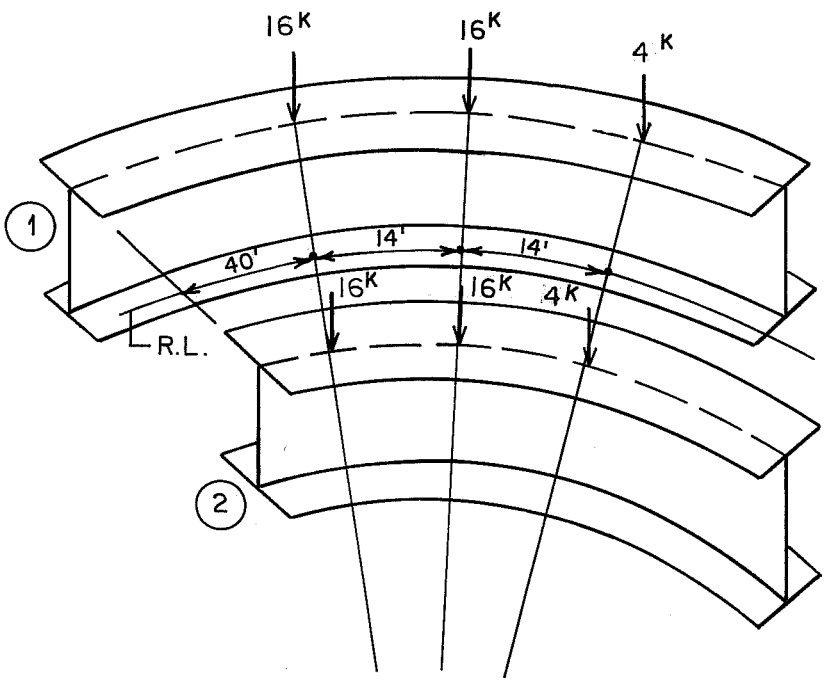
16K
16K
4K
1
40'
14'
14'
16K
16K
4K
R.L.
2

Table 4.2 Bending and Warping Stress in Bottom Flange (ksi)

a) Dead Load

SCHEME	RADIUS	D. SPACING	LOCATION*	GIRDER 1 V-LOAD	GIRDER 1 FEM	GIRDER 1 % D	GIRDER 2 V-LOAD	GIRDER 2 FEM	GIRDER 2 % D
A	1000 '	20 '	.5 L	28.06	30.82	-8.9	13.58	16.36	-17.0
B	1000 '	10 '	.45 L	24.96	27.26	-8.4	12.00	14.77	-18.7
C	500 '	20 '	.5 L	40.35	45.33	-11.0	7.27	13.09	-44.5
D	500 '	10 '	.45 L	32.71	37.71	-13.26	5.78	11.45	-49.5

b) Live Load

SCHEME	RADIUS	D. SPACING	LOCATION*	GIRDER 1 V-LOAD	GIRDER 1 FEM	GIRDER 1 % D	GIRDER 2 V-LOAD	GIRDER 2 FEM	GIRDER 2 % D
A	1000 '	20 '	.5 L	18.17	15.69	15.8	9.48	12.36	-23.3
B	1000 '	10 '	.45 L	15.25	13.48	13.1	7.84	10.54	-25.6
C	500 '	20 '	.5 L	26.97	20.77	29.8	6.26	13.01	-51.9
D	500 '	10 '	.45 L	20.01	16.33	22.5	4.43	10.06	-56.0

c) Dead Plus Live Load

SCHEME	RADIUS	D. SPACING	LOCATION*	GIRDER 1 V-LOAD	GIRDER 1 FEM	GIRDER 1 % D	GIRDER 2 V-LOAD	GIRDER 2 FEM	GIRDER 2 % D
A	1000 '	20 '	.5 L	46.23	46.51	-.6	23.06	28.72	-19.7
B	1000 '	10 '	.45 L	40.21	40.74	-1.3	19.83	25.31	-21.7
C	500 '	20 '	.5 L	67.32	66.10	1.8	13.53	26.10	-48.2
D	500 '	10 '	.45 L	52.72	54.04	-2.4	10.21	21.51	-52.5

*Location along span

Table 4.2 Bending and Warping Stress in Bottom Flange (ksi)

a) Dead Load

SCHEME	RADIUS	D. SPACING	LOCATION*	GIRDER 1 V-LOAD	GIRDER 1 FEM	GIRDER 1 % D	GIRDER 2 V-LOAD	GIRDER 2 FEM	GIRDER 2 % D
A	1000 '	20 '	.5 L	28.06	30.82	-8.9	13.58	16.36	-17.0
B	1000 '	10 '	.45 L	24.96	27.26	-8.4	12.00	14.77	-18.7
C	500 '	20 '	.5 L	40.35	45.33	-11.0	7.27	13.09	-44.5
D	500 '	10 '	.45 L	32.71	37.71	-13.26	5.78	11.45	-49.5

b) Live Load

SCHEME	RADIUS	D. SPACING	LOCATION*	GIRDER 1 V-LOAD	GIRDER 1 FEM	GIRDER 1 % D	GIRDER 2 V-LOAD	GIRDER 2 FEM	GIRDER 2 % D
A	1000 '	20 '	.5 L	18.17	15.69	15.8	9.48	12.36	-23.3
B	1000 '	10 '	.45 L	15.25	13.48	13.1	7.84	10.54	-25.6
C	500 '	20 '	.5 L	26.97	20.77	29.8	6.26	13.01	-51.9
D	500 '	10 '	.45 L	20.01	16.33	22.5	4.43	10.06	-56.0

c) Dead Plus Live Load

SCHEME	RADIUS	D. SPACING	LOCATION*	GIRDER 1 V-LOAD	GIRDER 1 FEM	GIRDER 1 % D	GIRDER 2 V-LOAD	GIRDER 2 FEM	GIRDER 2 % D
A	1000 '	20 '	.5 L	46.23	46.51	-.6	23.06	28.72	-19.7
B	1000 '	10 '	.45 L	40.21	40.74	-1.3	19.83	25.31	-21.7
C	500 '	20 '	.5 L	67.32	66.10	1.8	13.53	26.10	-48.2
D	500 '	10 '	.45 L	52.72	54.04	-2.4	10.21	21.51	-52.5

*Location along span

Table 4.1 Maximum Longitudinal Bending Stress in Bottom Flange (ksi)

a) Dead Load

SCHEME	RADIUS	D. SPACING	GIRDER 1			GIRDER 2		
			V-LOAD	FEM	% D	V-LOAD	FEM	% D
A	1000 '	20 '	24.21	23.87	1.4	11.74	11.95	-1.8
B	1000 '	10 '	24.37	23.61	3.2	11.58	11.78	-1.7
C	500 '	20 '	30.51	29.92	2.0	5.56	6.02	-7.6
D	500 '	10 '	30.82	29.62	4.1	5.25	5.87	-10.6

b) Live Load

SCHEME	RADIUS	D. SPACING	GIRDER 1			GIRDER 2		
			V-LOAD	FEM	% D	V-LOAD	FEM	% D
A	1000 '	20 '	14.63	12.38	18.2	7.60	9.70	-21.6
B	1000 '	10 '	14.70	12.34	19.1	7.53	9.57	-21.3
C	500 '	20 '	18.17	13.72	32.4	4.11	8.41	-51.1
D	500 '	10 '	18.32	13.76	33.1	3.97	8.21	-51.6

c) Dead Plus Live Load

SCHEME	RADIUS	D. SPACING	GIRDER 1			GIRDER 2		
			V-LOAD	FEM	% D	V-LOAD	FEM	% D
A	1000 '	20 '	38.84	36.25	7.1	19.34	21.65	-10.7
B	1000 '	10 '	39.07	35.95	8.7	19.11	21.34	-10.4
C	500 '	20 '	48.68	43.64	11.5	9.67	14.43	-33.0
D	500 '	10 '	49.14	43.88	12.0	9.22	14.10	-34.6

Table 4.1 Maximum Longitudinal Bending Stress in Bottom Flange (ksi)

a) Dead Load

SCHEME	RADIUS	D. SPACING	GIRDER 1 V-LOAD	GIRDER 1 FEM	GIRDER 1 % D	GIRDER 2 V-LOAD	GIRDER 2 FEM	GIRDER 2 % D
A	1000 '	20 '	24.21	23.87	1.4	11.74	11.95	-1.8
B	1000 '	10 '	24.37	23.61	3.2	11.58	11.78	-1.7
C	500 '	20 '	30.51	29.92	2.0	5.56	6.02	-7.6
D	500 '	10 '	30.82	29.62	4.1	5.25	5.87	-10.6

b) Live Load

SCHEME	RADIUS	D. SPACING	GIRDER 1 V-LOAD	GIRDER 1 FEM	GIRDER 1 % D	GIRDER 2 V-LOAD	GIRDER 2 FEM	GIRDER 2 % D
A	1000 '	20 '	14.63	12.38	18.2	7.60	9.70	-21.6
B	1000 '	10 '	14.70	12.34	19.1	7.53	9.57	-21.3
C	500 '	20 '	18.17	13.72	32.4	4.11	8.41	-51.1
D	500 '	10 '	18.32	13.76	33.1	3.97	8.21	-51.6

c) Dead Plus Live Load

SCHEME	RADIUS	D. SPACING	GIRDER 1 V-LOAD	GIRDER 1 FEM	GIRDER 1 % D	GIRDER 2 V-LOAD	GIRDER 2 FEM	GIRDER 2 % D
A	1000 '	20 '	38.84	36.25	7.1	19.34	21.65	-10.7
B	1000 '	10 '	39.07	35.95	8.7	19.11	21.34	-10.4
C	500 '	20 '	48.68	43.64	11.5	9.67	14.43	-33.0
D	500 '	10 '	49.14	43.88	12.0	9.22	14.10	-34.6

Table 4.6 Bending and Warping Stress in Bottom Flange (ksi)

a) Dead Load

BRIDGE	R.L. RADIUS	D. SPNG.	SKEW	LOCATION	GIRDER 1 V-LOAD	GIRDER 1 FEM	GIRDER 1 % D	GIRDER 4 V-LOAD	GIRDER 4 FEM	GIRDER 4 % D
1	175 '	10.46'	NO	.096 L	7.98	7.96	.3	2.87	3.01	-4.7
				.288 L	-7.41	-7.48	-.9	-4.36	-4.87	-10.5
2	175 '	20.92'	NO	.096 L	8.30	4.89	69.7	2.00	1.66	20.5
				.288 L	-8.47	-7.84	8.0	-4.78	-5.03	-5.0
3	350 '	10.46'	NO	.096 L	6.04	6.17	-2.1	3.72	3.84	-3.1
				.288 L	-6.03	-6.14	-1.8	-4.66	-4.77	-2.3
4	175 '	10.46'	2 TO 30°	.096 L	10.54	10.16	3.7	1.56	2.19	-28.8
			3 TO -4°	.288 L	-1.89	-4.07	-53.6	-4.47	-7.09	-37.0

b) Live Load, Outer Load Position

BRIDGE	R.L. RADIUS	D. SPNG.	SKEW	LOCATION	GIRDER 1 V-LOAD	GIRDER 1 FEM	GIRDER 1 % D	GIRDER 4 V-LOAD	GIRDER 4 FEM	GIRDER 4 % D
1	175 '	10.46'	NO	.135 L	7.93	7.49	5.9	-1.48	-1.64	-9.8
				.327 L	-2.32	-2.36	-1.7	.33	.34	-2.9
2	175 '	20.92'	NO	.135 L	7.50	8.92	-15.9	-1.48	-1.32	12.1
				.327 L	-2.55	-3.03	-15.8	.29	.20	45.0
3	350 '	10.46'	NO	.135 L	6.29	6.15	2.3	-.69	-1.07	-35.5
				.327 L	-1.90	-1.91	-.5	.16	.28	-42.9
4	175 '	10.46'	2 TO 30°	.135 L	8.81	7.07	24.6	-1.62	-1.54	5.2
			3 TO -4°	.327 L	-2.42	-1.15	110.4	.39	.38	2.6

c) Live Load, Middle Load Position

BRIDGE	R.L. RADIUS	D. SPNG.	SKEW	LOCATION	GIRDER 1 V-LOAD	GIRDER 1 FEM	GIRDER 1 % D	GIRDER 4 V-LOAD	GIRDER 4 FEM	GIRDER 4 % D
1	175 '	10.46'	NO	.135 L	1.64	4.16	-60.6	-1.42	1.28	-210.9
				.327 L	-.36	-1.26	-71.4	.31	-.53	-158.5
2	175 '	20.92'	NO	.135 L	2.30	4.75	-51.6	-1.44	1.54	-193.5
				.327 L	-.37	-1.64	-77.4	.28	-.74	-137.8
3	350 '	10.46'	NO	.135 L	.72	3.10	-76.8	-.68	1.79	-138.0
				.327 L	-.17	-.93	-81.7	.15	-.59	-125.4
4	175 '	10.46'	2 TO 30°	.135 L	1.79	3.97	-54.9	-1.46	1.17	-224.8
			3 TO -4°	.327 L	-.30	-1.10	-72.7	.35	-.95	-136.8

Table 4.6 Bending and Warping Stress in Bottom Flange (ksi)

a) Dead Load

BRIDGE	R.L. RADIUS	D. SPNG.	SKEW	LOCATION	GIRDER 1 V-LOAD	GIRDER 1 FEM	GIRDER 1 % D	GIRDER 4 V-LOAD	GIRDER 4 FEM	GIRDER 4 % D
1	175 '	10.46'	NO	.096 L	7.98	7.96	.3	2.87	3.01	-4.7
				.288 L	-7.41	-7.48	-.9	-4.36	-4.87	-10.5
2	175 '	20.92'	NO	.096 L	8.30	4.89	69.7	2.00	1.66	20.5
				.288 L	-8.47	-7.84	8.0	-4.78	-5.03	-5.0
3	350 '	10.46'	NO	.096 L	6.04	6.17	-2.1	3.72	3.84	-3.1
				.288 L	-6.03	-6.14	-1.8	-4.66	-4.77	-2.3
4	175 '	10.46'	2 TO 30°	.096 L	10.54	10.16	3.7	1.56	2.19	-28.8
			3 TO -4°	.288 L	-1.89	-4.07	-53.6	-4.47	-7.09	-37.0

b) Live Load, Outer Load Position

BRIDGE	R.L. RADIUS	D. SPNG.	SKEW	LOCATION	GIRDER 1 V-LOAD	GIRDER 1 FEM	GIRDER 1 % D	GIRDER 4 V-LOAD	GIRDER 4 FEM	GIRDER 4 % D
1	175 '	10.46'	NO	.135 L	7.93	7.49	5.9	-1.48	-1.64	-9.8
				.327 L	-2.32	-2.36	-1.7	.33	.34	-2.9
2	175 '	20.92'	NO	.135 L	7.50	8.92	-15.9	-1.48	-1.32	12.1
				.327 L	-2.55	-3.03	-15.8	.29	.20	45.0
3	350 '	10.46'	NO	.135 L	6.29	6.15	2.3	-.69	-1.07	-35.5
				.327 L	-1.90	-1.91	-.5	.16	.28	-42.9
4	175 '	10.46'	2 TO 30°	.135 L	8.81	7.07	24.6	-1.62	-1.54	5.2
			3 TO -4°	.327 L	-2.42	-1.15	110.4	.39	.38	2.6

c) Live Load, Middle Load Position

BRIDGE	R.L. RADIUS	D. SPNG.	SKEW	LOCATION	GIRDER 1 V-LOAD	GIRDER 1 FEM	GIRDER 1 % D	GIRDER 4 V-LOAD	GIRDER 4 FEM	GIRDER 4 % D
1	175 '	10.46'	NO	.135 L	1.64	4.16	-60.6	-1.42	1.28	-210.9
				.327 L	-.36	-1.26	-71.4	.31	-.53	-158.5
2	175 '	20.92'	NO	.135 L	2.30	4.75	-51.6	-1.44	1.54	-193.5
				.327 L	-.37	-1.64	-77.4	.28	-.74	-137.8
3	350 '	10.46'	NO	.135 L	.72	3.10	-76.8	-.68	1.79	-138.0
				.327 L	-.17	-.93	-81.7	.15	-.59	-125.4
4	175 '	10.46'	2 TO 30°	.135 L	1.79	3.97	-54.9	-1.46	1.17	-224.8
			3 TO -4°	.327 L	-.30	-1.10	-72.7	.35	-.95	-136.8

Table 4.4 Longitudinal Bending Stress in Bottom Flange (ksi)

a) Dead Load

BRIDGE	R.L. RADIUS	D. SPACING	SKEW	LOCATION*	GIRDER 1 V-LOAD	GIRDER 1 FEM	GIRDER 1 % D	GIRDER 2 V-LOAD	GIRDER 2 FEM	GIRDER 2 % D	GIRDER 3 V-LOAD	GIRDER 3 FEM	GIRDER 3 % D	GIRDER 4 V-LOAD	GIRDER 4 FEM	GIRDER 4 % D
1	175 '	10.46'	NO	.115 L	7.20	6.52	9.4	5.56	5.24	6.1	4.03	5.24	3.3	2.61	2.31	13.0
				.307 L	-8.71	-7.47	14.2	-7.57	-6.90	9.7	-6.50	-6.90	6.2	-5.49	-5.29	3.8
2	175 '	20.92'	NO	.115 L	7.04	6.48	8.6	5.46	5.03	8.5	3.99	3.95	1.0	2.62	2.34	12.0
				.307 L	-8.88	-8.38	6.0	-7.63	-6.64	14.9	-6.44	-5.71	12.8	-5.33	-4.79	11.3
3	350 '	10.46'	NO	.115 L	5.78	5.57	3.8	5.02	4.88	2.9	4.28	4.20	1.9	3.57	3.45	3.5
				.307 L	-7.63	-6.65	14.7	-7.09	-6.36	11.5	-6.57	-5.88	11.7	-6.07	-5.47	11.0
4	175 '	10.46'	2 TO 30°	.115 L	9.98	8.45	18.1	6.89	6.33	8.8	3.95	3.99	-1.0	1.16	1.21	-4.1
			3 TO -4°	.307 L	-5.42	-5.18	4.6	-5.80	-5.92	-2.0	-6.18	-5.10	21.2	-4.46	-4.15	7.5

b) Live Load, Outer Load Position

BRIDGE	R.L. RADIUS	D. SPACING	SKEW	LOCATION*	GIRDER 1 V-LOAD	GIRDER 1 FEM	GIRDER 1 % D	GIRDER 4 V-LOAD	GIRDER 4 FEM	GIRDER 4 % D
1	175 '	10.46'	NO	.135 L	6.89	5.84	18.0	-1.31	-1.45	-9.7
				.327 L	-2.05	-1.84	11.4	.30	.18	66.7
2	175 '	20.92'	NO	.135 L	6.81	5.37	26.8	-1.34	-1.18	13.6
				.327 L	-2.03	-1.87	8.6	.29	.12	141.7
3	350 '	10.46'	NO	.135 L	5.87	5.27	11.4	-.65	-.80	-18.8
				.327 L	-1.79	-1.61	11.2	.15	.14	7.1
4	175 '	10.46'	2 TO 30°	.135 L	7.66	5.51	39.0	-1.44	-1.35	6.7
			3 TO -4°	.327 L	-2.28	-.98	132.7	.32	.19	68.4

c) Live Load, Middle Load Position

BRIDGE	R.L. RADIUS	D. SPACING	SKEW	LOCATION*	GIRDER 1 V-LOAD	GIRDER 1 FEM	GIRDER 1 % D	GIRDER 4 V-LOAD	GIRDER 4 FEM	GIRDER 4 % D
1	175 '	10.46'	NO	.135 L	1.43	3.33	-57.1	-1.26	.91	-238.5
				.327 L	-.32	-1.01	-68.3	.28	-.40	-171.0
2	175 '	20.92'	NO	.135 L	1.46	2.99	-51.2	-1.29	.89	-244.9
				.327 L	-.31	-1.01	-69.3	.28	-.47	-160.0
3	350 '	10.46 '	NO	.135 L	.67	2.76	-75.7	-.64	1.53	-141.8
				.327 L	-.16	-.82	-80.5	.14	-.51	-127.5
4	175 '	10.46'	2 TO 30°	.135 L	1.57	3.18	-50.6	-1.30	.82	-258.5
			3 TO -4°	.327 L	-.29	-.78	-62.8	.31	-.49	-163.3

* LOCATION FROM FIRST SUPPORT, WHERE L IS GIRDER LENGTH

Table 4.4 Longitudinal Bending Stress in Bottom Flange (ksi)

a) Dead Load

BRIDGE	R.L. RADIUS	D. SPACING	SKEW	LOCATION*	GIRDER 1 V-LOAD	GIRDER 1 FEM	GIRDER 1 % D	GIRDER 2 V-LOAD	GIRDER 2 FEM	GIRDER 2 % D	GIRDER 3 V-LOAD	GIRDER 3 FEM	GIRDER 3 % D	GIRDER 4 V-LOAD	GIRDER 4 FEM	GIRDER 4 % D
1	175 '	10.46'	NO	.115 L	7.20	6.52	9.4	5.56	5.24	6.1	4.03	5.24	3.3	2.61	2.31	13.0
				.307 L	-8.71	-7.47	14.2	-7.57	-6.90	9.7	-6.50	-6.90	6.2	-5.49	-5.29	3.8
2	175 '	20.92'	NO	.115 L	7.04	6.48	8.6	5.46	5.03	8.5	3.99	3.95	1.0	2.62	2.34	12.0
				.307 L	-8.88	-8.38	6.0	-7.63	-6.64	14.9	-6.44	-5.71	12.8	-5.33	-4.79	11.3
3	350 '	10.46'	NO	.115 L	5.78	5.57	3.8	5.02	4.88	2.9	4.28	4.20	1.9	3.57	3.45	3.5
				.307 L	-7.63	-6.65	14.7	-7.09	-6.36	11.5	-6.57	-5.88	11.7	-6.07	-5.47	11.0
4	175 '	10.46'	2 TO 30°	.115 L	9.98	8.45	18.1	6.89	6.33	8.8	3.95	3.99	-1.0	1.16	1.21	-4.1
			3 TO -4°	.307 L	-5.42	-5.18	4.6	-5.80	-5.92	-2.0	-6.18	-5.10	21.2	-4.46	-4.15	7.5

b) Live Load, Outer Load Position

BRIDGE	R.L. RADIUS	D. SPACING	SKEW	LOCATION*	GIRDER 1 V-LOAD	GIRDER 1 FEM	GIRDER 1 % D	GIRDER 4 V-LOAD	GIRDER 4 FEM	GIRDER 4 % D
1	175 '	10.46'	NO	.135 L	6.89	5.84	18.0	-1.31	-1.45	-9.7
				.327 L	-2.05	-1.84	11.4	.30	.18	66.7
2	175 '	20.92'	NO	.135 L	6.81	5.37	26.8	-1.34	-1.18	13.6
				.327 L	-2.03	-1.87	8.6	.29	.12	141.7
3	350 '	10.46'	NO	.135 L	5.87	5.27	11.4	-.65	-.80	-18.8
				.327 L	-1.79	-1.61	11.2	.15	.14	7.1
4	175 '	10.46'	2 TO 30°	.135 L	7.66	5.51	39.0	-1.44	-1.35	6.7
			3 TO -4°	.327 L	-2.28	-.98	132.7	.32	.19	68.4

c) Live Load, Middle Load Position

BRIDGE	R.L. RADIUS	D. SPACING	SKEW	LOCATION*	GIRDER 1 V-LOAD	GIRDER 1 FEM	GIRDER 1 % D	GIRDER 4 V-LOAD	GIRDER 4 FEM	GIRDER 4 % D
1	175 '	10.46'	NO	.135 L	1.43	3.33	-57.1	-1.26	.91	-238.5
				.327 L	-.32	-1.01	-68.3	.28	-.40	-171.0
2	175 '	20.92'	NO	.135 L	1.46	2.99	-51.2	-1.29	.89	-244.9
				.327 L	-.31	-1.01	-69.3	.28	-.47	-160.0
3	350 '	10.46 '	NO	.135 L	.67	2.76	-75.7	-.64	1.53	-141.8
				.327 L	-.16	-.82	-80.5	.14	-.51	-127.5
4	175 '	10.46'	2 TO 30°	.135 L	1.57	3.18	-50.6	-1.30	.82	-258.5
			3 TO -4°	.327 L	-.29	-.78	-62.8	.31	-.49	-163.3

* LOCATION FROM FIRST SUPPORT, WHERE L IS GIRDER LENGTH

Table 4.5 Warping Stress in Bottom Flange (ksi)

a) Dead Load

BRIDGE	R.L. RADIUS	D. SPNG.	SKEW	LOCATION	GIRDER 1 V-LOAD	GIRDER 1 FEM	GIRDER 1 % D	GIRDER 4 V-LOAD	GIRDER 4 FEM	GIRDER 4 % D
1	175 '	10.46'	NO	.096 L	-.89	-1.57	-43.3	-.29	-.73	-60.3
				.288 L	.87	1.37	-36.5	.46	.87	-47.1
2	175 '	20.92'	NO	.096 L	-1.26	-1.30	-3.1	-.47	-.54	-12.9
				.288 L	2.62	2.38	10.1	1.38	1.52	-9.2
3	350 '	10.46'	NO	.096 L	-.35	-.71	-50.7	-.20	-.45	-55.6
				.288 L	.36	.63	-42.9	.27	.49	-44.9
4	175 '	10.46'	2 TO 30°	.096 L	-1.17	-2.07	-43.5	-.15	-.80	-81.3
			3 TO -4°	.288 L	-.44	-1.11	-60.4	-.65	-3.07	-78.8

b) Live Load, Outer Load Position

BRIDGE	R.L. RADIUS	D. SPNG.	SKEW	LOCATION	GIRDER 1 V-LOAD	GIRDER 1 FEM	GIRDER 1 % D	GIRDER 4 V-LOAD	GIRDER 4 FEM	GIRDER 4 % D
1	175 '	10.46'	NO	.135 L	-1.04	-1.65	-37.0	.17	-.19	-189.5
				.327 L	.27	.52	-48.1	-.03	.16	-118.8
2	175 '	20.92'	NO	.135 L	.69	-3.55	80.6	.14	.14	0
				.327 L	.52	1.16	-55.2	0.0	.08	-100.0
3	350 '	10.46'	NO	.135 L	-.42	-.88	-52.3	.04	-.27	85.2
				.327 L	.11	.30	-63.3	-.01	.14	-107.1
4	175 '	10.46'	2 TO 30°	.135 L	-1.15	-1.56	-26.3	.18	-.19	-194.7
			3 TO -4°	.327 L	.14	-.17	-182.4	-.07	.19	-136.8

c) Live Load, Middle Load Position

BRIDGE	R.L. RADIUS	D. SPNG.	SKEW	LOCATION	GIRDER 1 V-LOAD	GIRDER 1 FEM	GIRDER 1 % D	GIRDER 4 V-LOAD	GIRDER 4 FEM	GIRDER 4 % D
1	175 '	10.46'	NO	.135 L	-.21	-.83	-74.7	.16	-.37	-143.2
				.327 L	.04	.25	-84.0	-.03	.13	-123.1
2	175 '	20.92'	NO	.135 L	.84	-1.76	-147.7	.15	-.65	-123.1
				.327 L	-.06	.63	-109.5	0.0	.27	-100.0
3	350 '	10.46'	NO	.135 L	-.05	-.34	-85.3	.04	-.26	-115.4
				.327 L	.01	.11	-90.9	-.01	.08	-112.5
4	175 '	10.46'	2 TO 30°	.135 L	-.22	-.79	-72.2	.16	-.35	-145.7
			3 TO -4°	.327 L	.01	-.32	-103.1	-.04	.46	-108.7

Table 4.5 Warping Stress in Bottom Flange (ksi)

a) Dead Load

BRIDGE	R.L. RADIUS	D. SPNG.	SKEW	LOCATION	GIRDER 1 V-LOAD	GIRDER 1 FEM	GIRDER 1 % D	GIRDER 4 V-LOAD	GIRDER 4 FEM	GIRDER 4 % D
1	175 '	10.46'	NO	.096 L	-.89	-1.57	-43.3	-.29	-.73	-60.3
				.288 L	.87	1.37	-36.5	.46	.87	-47.1
2	175 '	20.92'	NO	.096 L	-1.26	-1.30	-3.1	-.47	-.54	-12.9
				.288 L	2.62	2.38	10.1	1.38	1.52	-9.2
3	350 '	10.46'	NO	.096 L	-.35	-.71	-50.7	-.20	-.45	-55.6
				.288 L	.36	.63	-42.9	.27	.49	-44.9
4	175 '	10.46'	2 TO 30°	.096 L	-1.17	-2.07	-43.5	-.15	-.80	-81.3
			3 TO -4°	.288 L	-.44	-1.11	-60.4	-.65	-3.07	-78.8

b) Live Load, Outer Load Position

BRIDGE	R.L. RADIUS	D. SPNG.	SKEW	LOCATION	GIRDER 1 V-LOAD	GIRDER 1 FEM	GIRDER 1 % D	GIRDER 4 V-LOAD	GIRDER 4 FEM	GIRDER 4 % D
1	175 '	10.46'	NO	.135 L	-1.04	-1.65	-37.0	.17	-.19	-189.5
				.327 L	.27	.52	-48.1	-.03	.16	-118.8
2	175 '	20.92'	NO	.135 L	.69	-3.55	80.6	.14	.14	0
				.327 L	.52	1.16	-55.2	0.0	.08	-100.0
3	350 '	10.46'	NO	.135 L	-.42	-.88	-52.3	.04	-.27	85.2
				.327 L	.11	.30	-63.3	-.01	.14	-107.1
4	175 '	10.46'	2 TO 30°	.135 L	-1.15	-1.56	-26.3	.18	-.19	-194.7
			3 TO -4°	.327 L	.14	-.17	-182.4	-.07	.19	-136.8

c) Live Load, Middle Load Position

BRIDGE	R.L. RADIUS	D. SPNG.	SKEW	LOCATION	GIRDER 1 V-LOAD	GIRDER 1 FEM	GIRDER 1 % D	GIRDER 4 V-LOAD	GIRDER 4 FEM	GIRDER 4 % D
1	175 '	10.46'	NO	.135 L	-.21	-.83	-74.7	.16	-.37	-143.2
				.327 L	.04	.25	-84.0	-.03	.13	-123.1
2	175 '	20.92'	NO	.135 L	.84	-1.76	-147.7	.15	-.65	-123.1
				.327 L	-.06	.63	-109.5	0.0	.27	-100.0
3	350 '	10.46'	NO	.135 L	-.05	-.34	-85.3	.04	-.26	-115.4
				.327 L	.01	.11	-90.9	-.01	.08	-112.5
4	175 '	10.46'	2 TO 30°	.135 L	-.22	-.79	-72.2	.16	-.35	-145.7
			3 TO -4°	.327 L	.01	-.32	-103.1	-.04	.46	-108.7

4.39

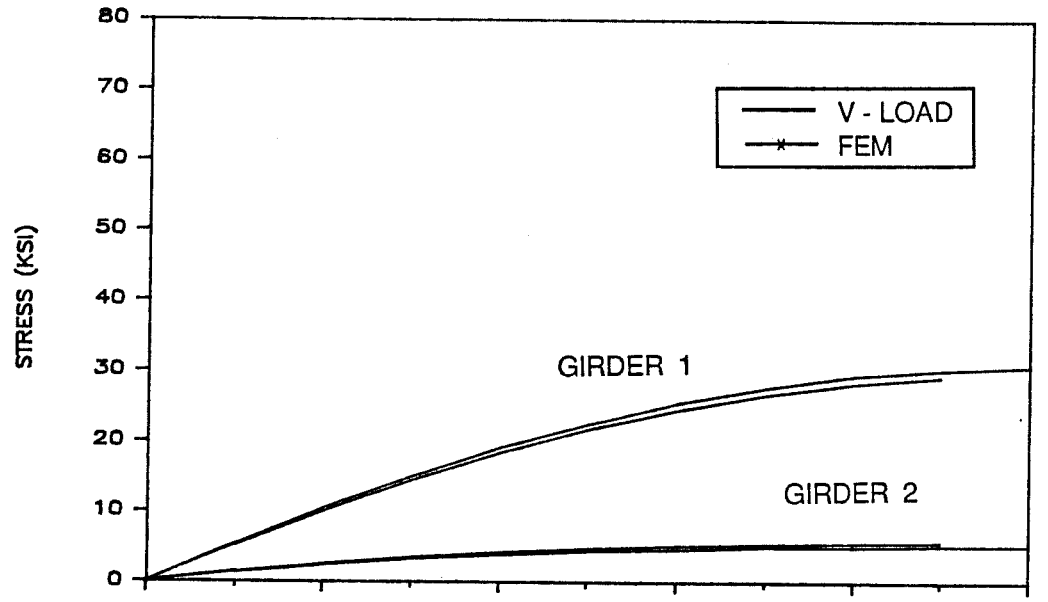
80
70
60
50
40
30
20
10
0
STRESS (KSI)
V - LOAD
FEM
GIRDER 1
GIRDER 2

D

4.36

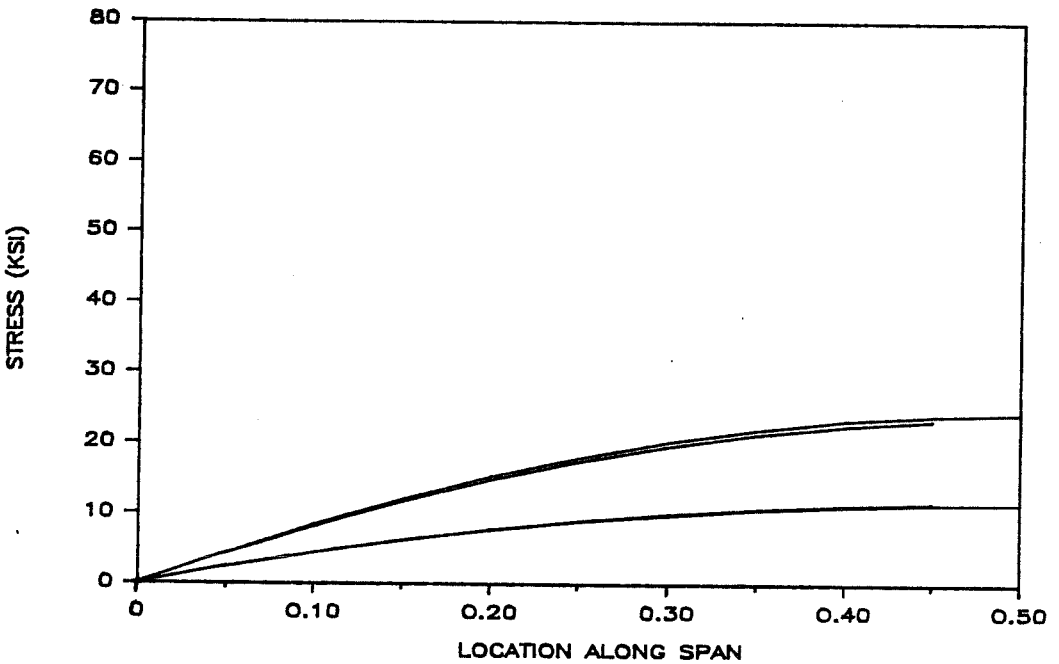
80
70
60
50
40
30
20
10
0
STRESS (KSI)
0
0.10
0.20
0.30
0.40
0.50
LOCATION ALONG SPAN

B

4.49

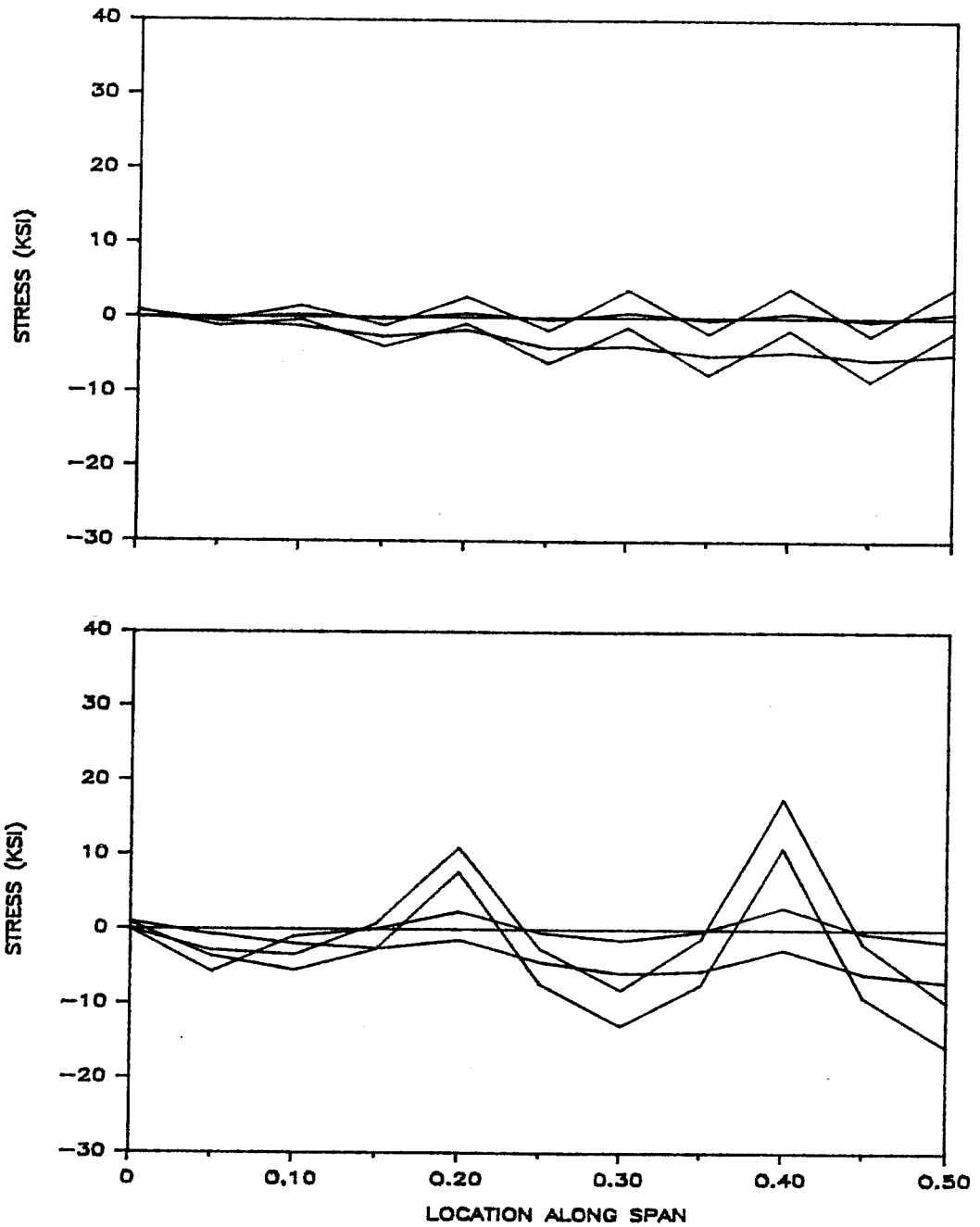
40
30
20
10
0
−10
−20
−30
STRESS (KSI)
40
30
20
10
0
−10
−20
−30
STRESS (KSI)
0
0.10
0.20
0.30
0.40
0.50
LOCATION ALONG SPAN

4.49

4.59

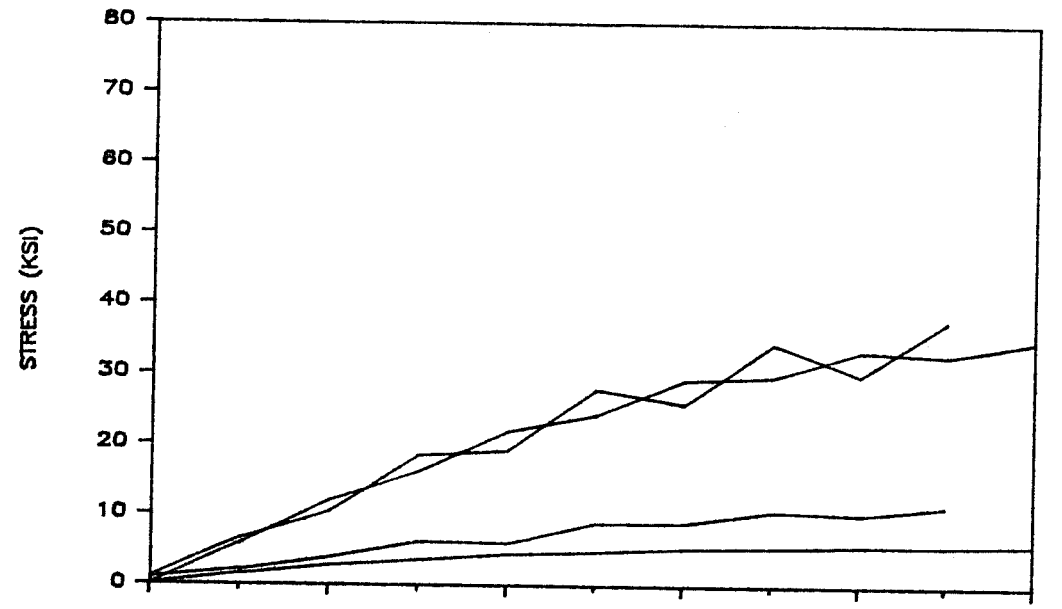
STRESS (KSI)
80
70
60
50
40
30
20
10
0

D
10'

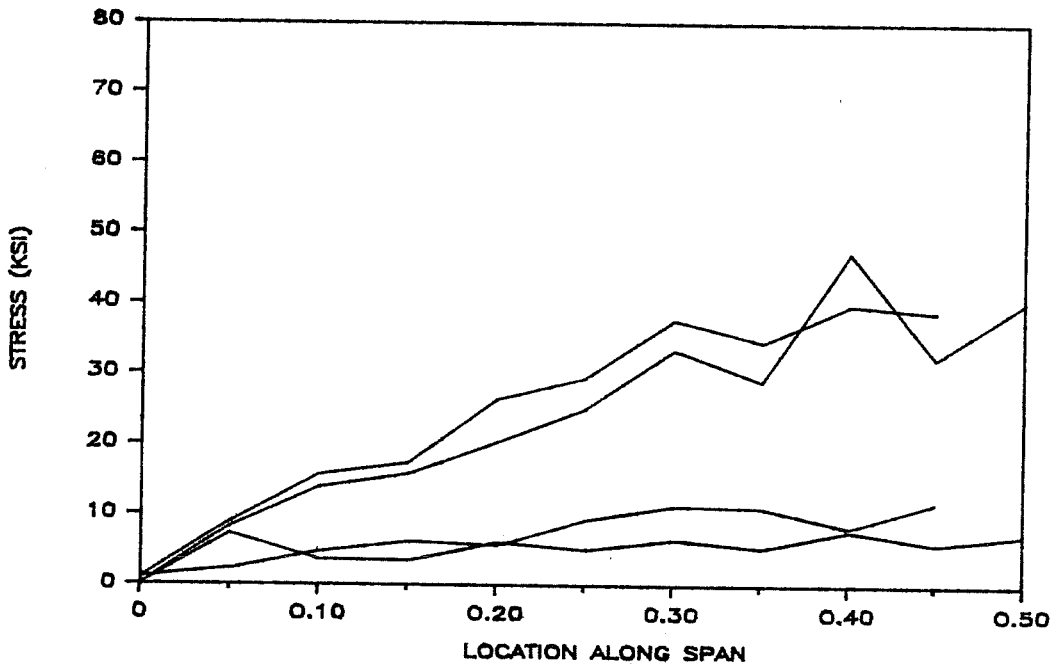
STRESS (KSI)
80
70
60
50
40
30
20
10
0
0
0.10
0.20
0.30
0.40
0.50
LOCATION ALONG SPAN

C
20'

4.6a

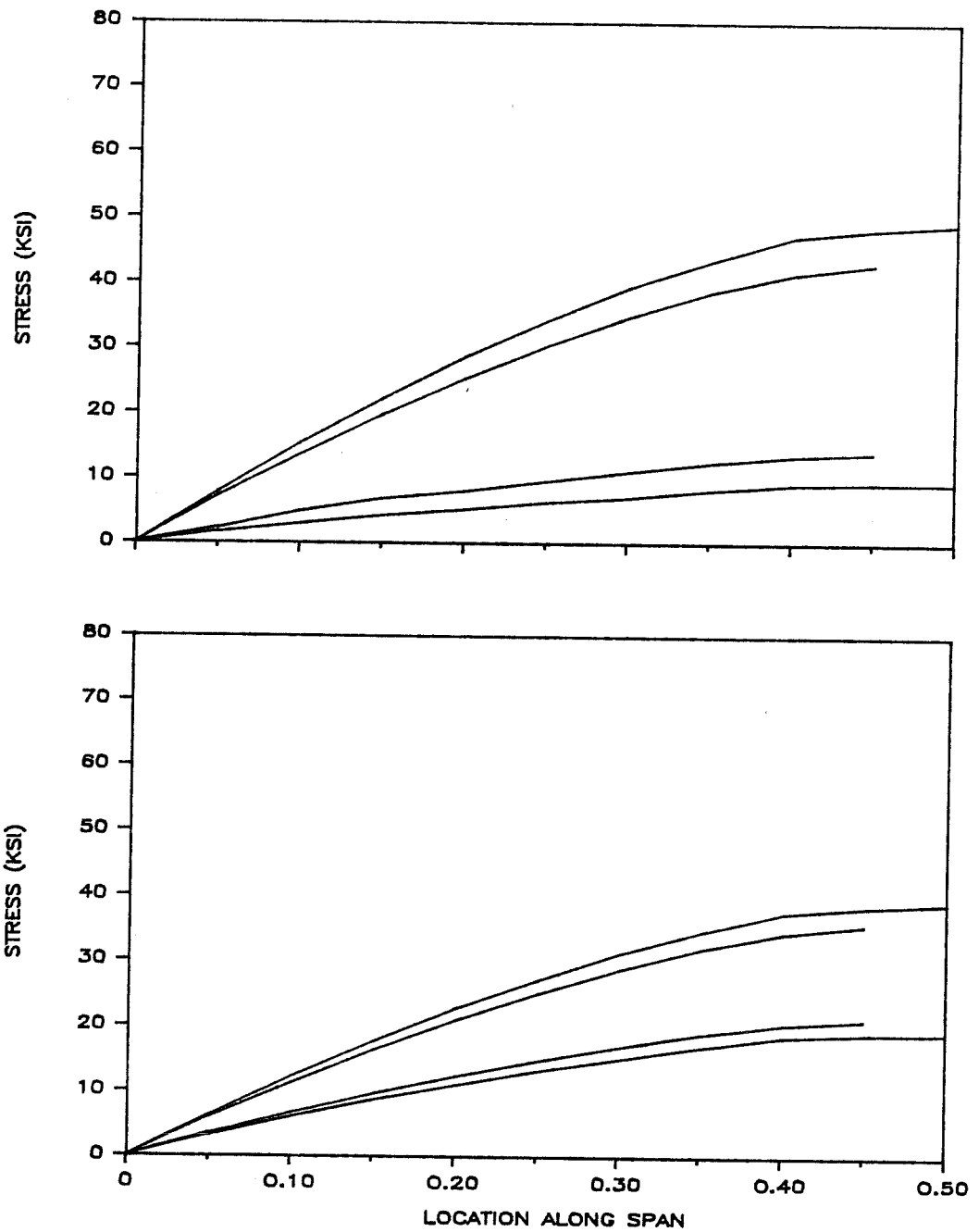
80
70
60
50
40
30
20
10
0
STRESS (KSI)
D
b
80
70
60
50
40
30
20
10
0
STRESS (KSI)
B
0
0.10
0.20
0.30
0.40
0.50
LOCATION ALONG SPAN

4.7a

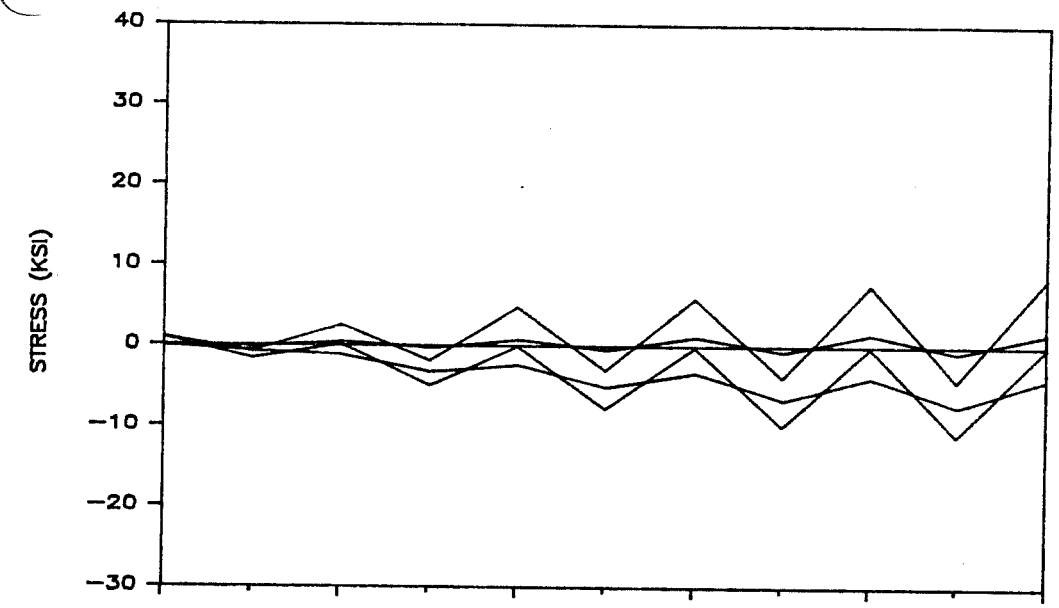
40
30
20
10
0
−10
−20
−30
STRESS (KSI)

D

4.7b

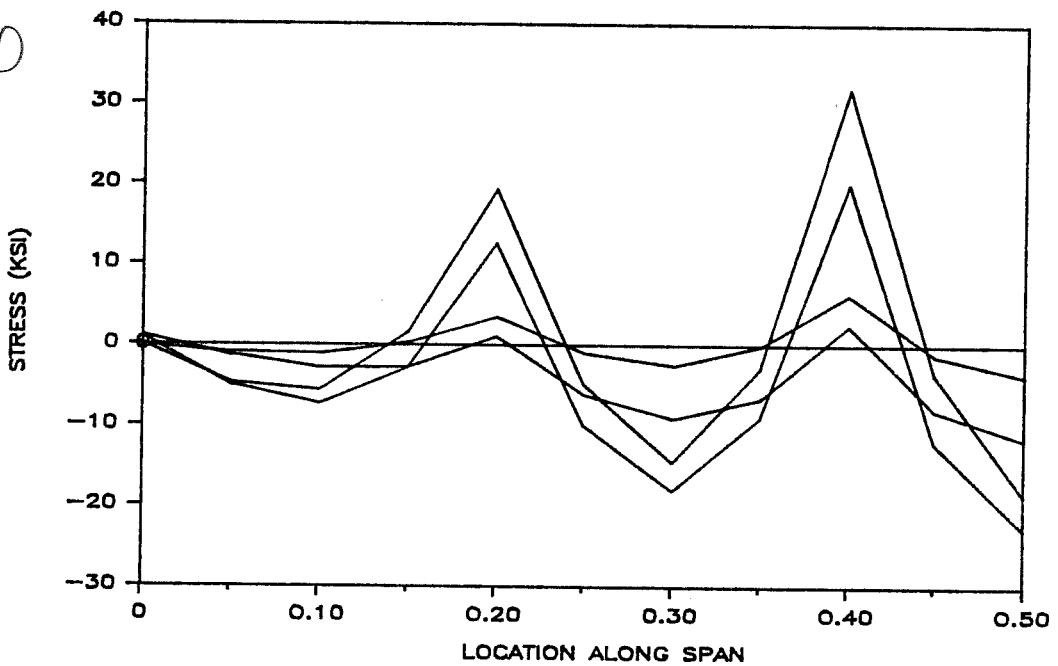
40
30
20
10
0
−10
−20
−30
STRESS (KSI)
0
0.10
0.20
0.30
0.40
0.50
LOCATION ALONG SPAN

C

4.8a

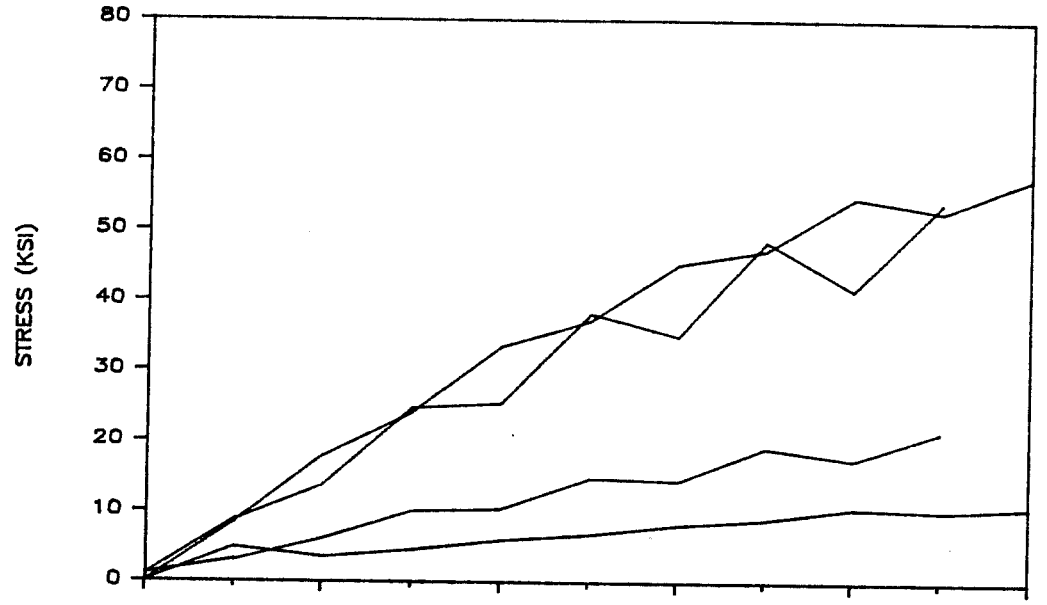
STRESS (KSI)
80
70
60
50
40
30
20
10
0

D

4.8b

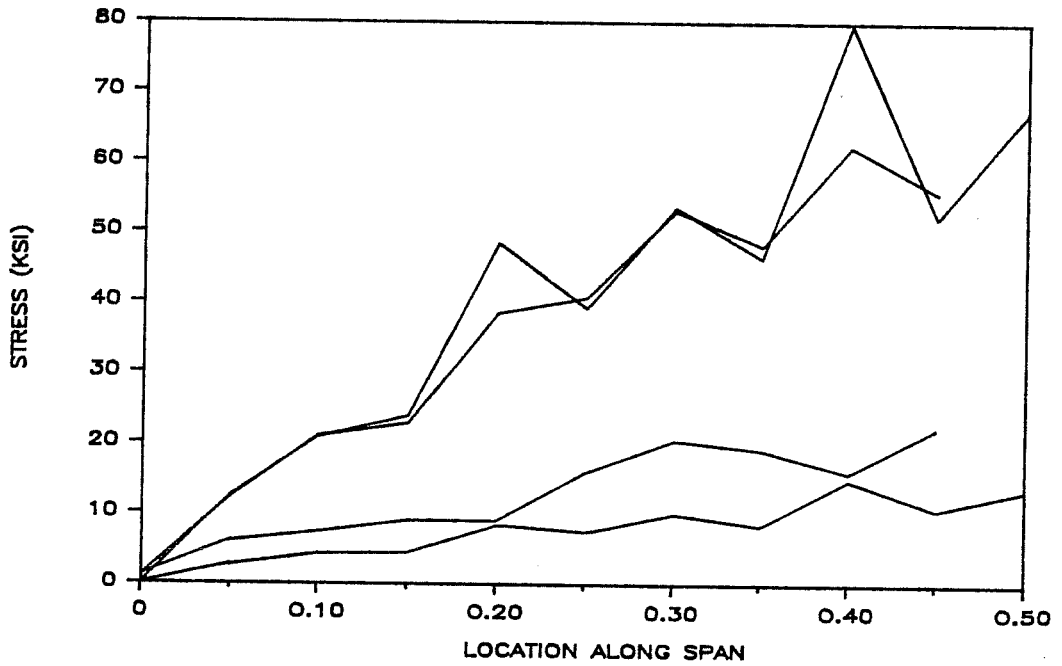
STRESS (KSI)
80
70
60
50
40
30
20
10
0
0
0.10
0.20
0.30
0.40
0.50
LOCATION ALONG SPAN

C

4.13a

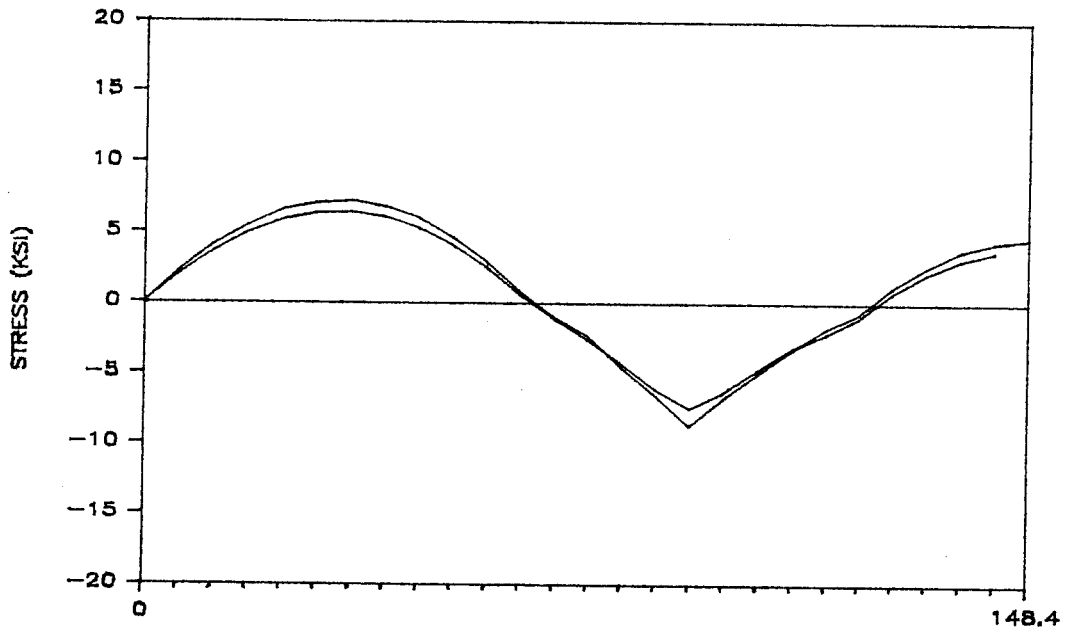
20
15
10
5
0
−5
−10
−15
−20
STRESS (KSI)
0
148.4

b

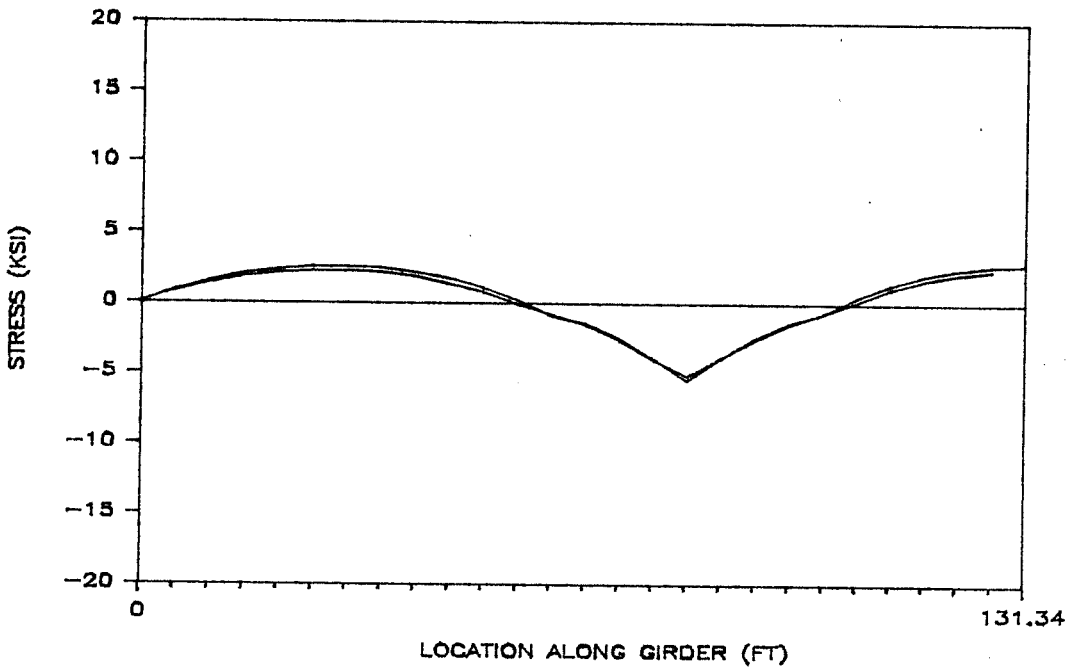
20
15
10
5
0
−5
−10
−15
−20
STRESS (KSI)
0
131.34
LOCATION ALONG GIRDER (FT)

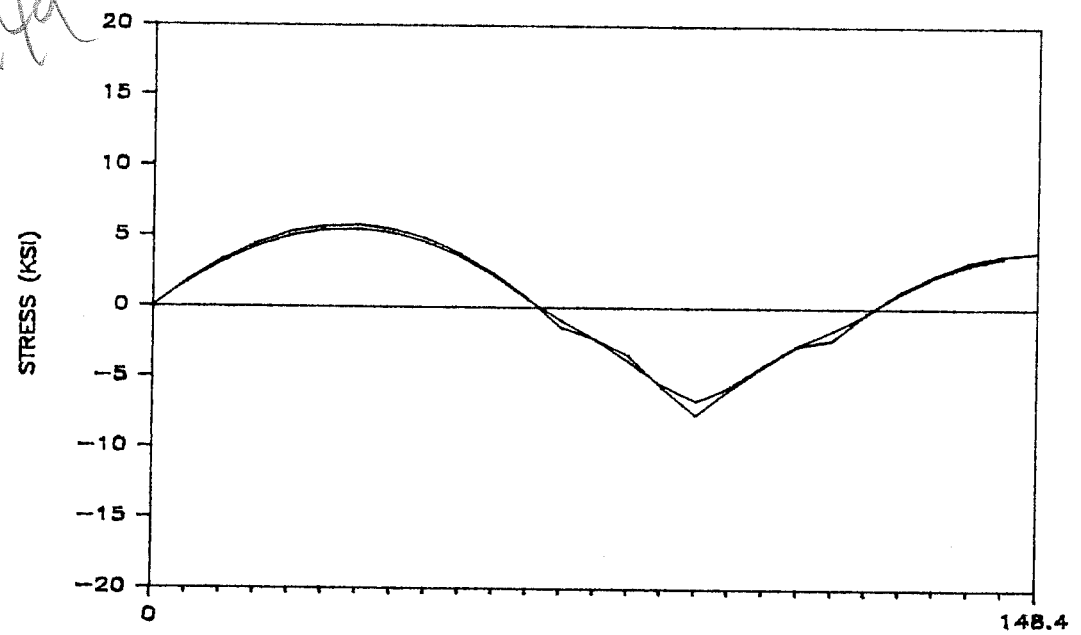
20
15
10
5
0
−5
−10
−15
−20
STRESS (KSI)
0
148.4

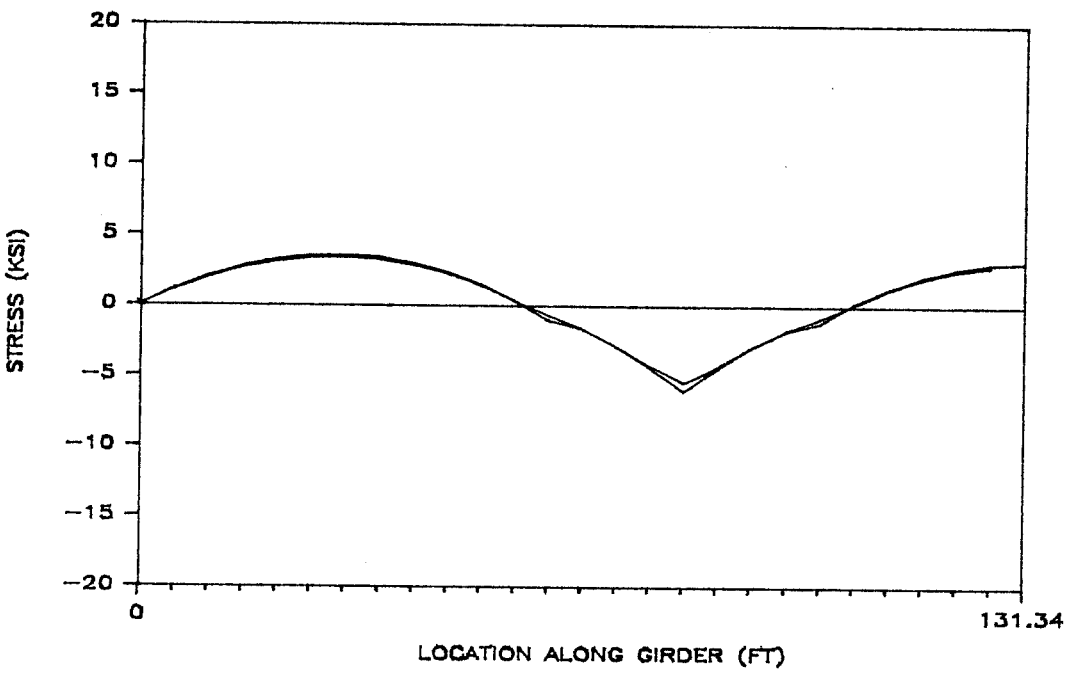
20
15
10
5
0
−5
−10
−15
−20
STRESS (KSI)
0
131.34
LOCATION ALONG GIRDER (FT)

B1

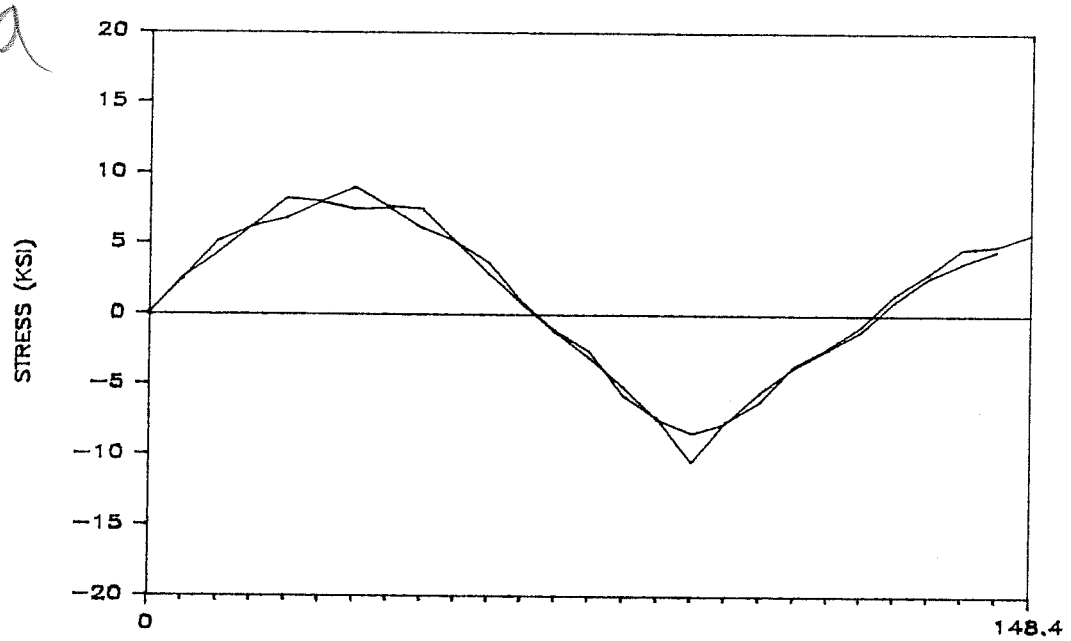
20
15
10
5
0
−5
−10
−15
−20
STRESS (KSI)
0
148.4

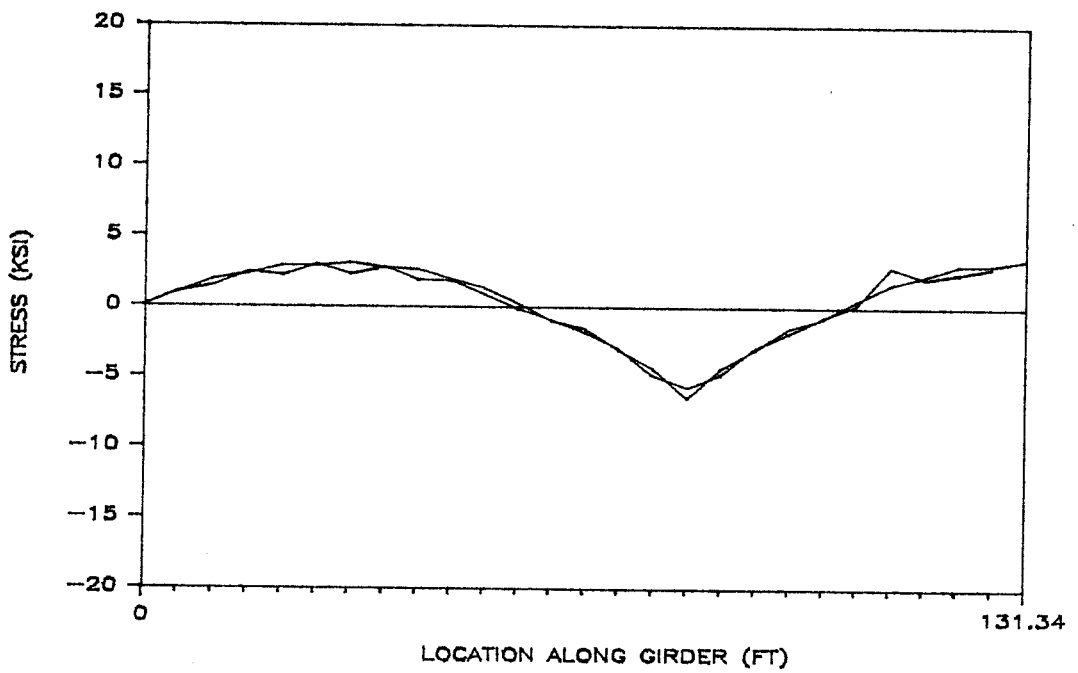
20
15
10
5
0
−5
−10
−15
−20
STRESS (KSI)
0
131.34
LOCATION ALONG GIRDER (FT)

B3

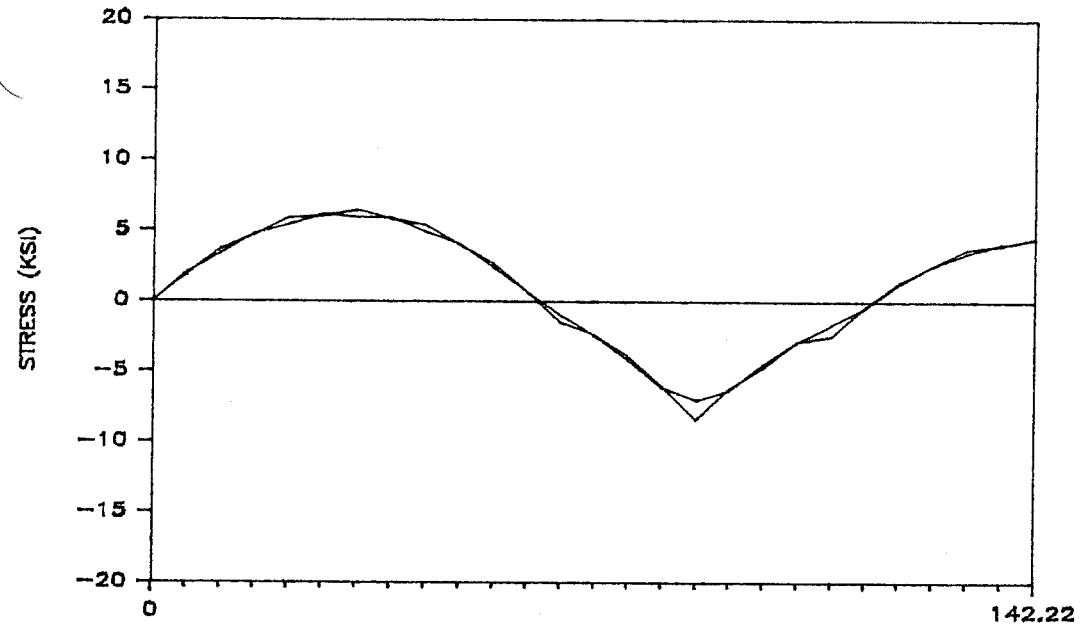
20
15
10
5
0
−5
−10
−15
−20
STRESS (KSI)
0
142.22

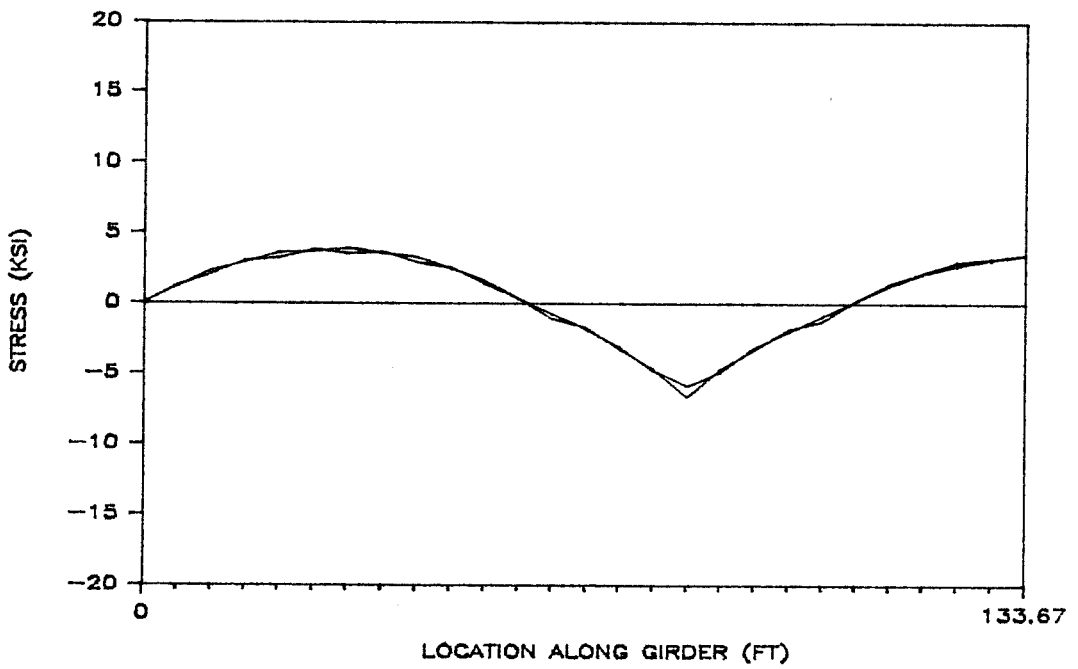
20
15
10
5
0
−5
−10
−15
−20
STRESS (KSI)
0
133.67
LOCATION ALONG GIRDER (FT)

4.17a

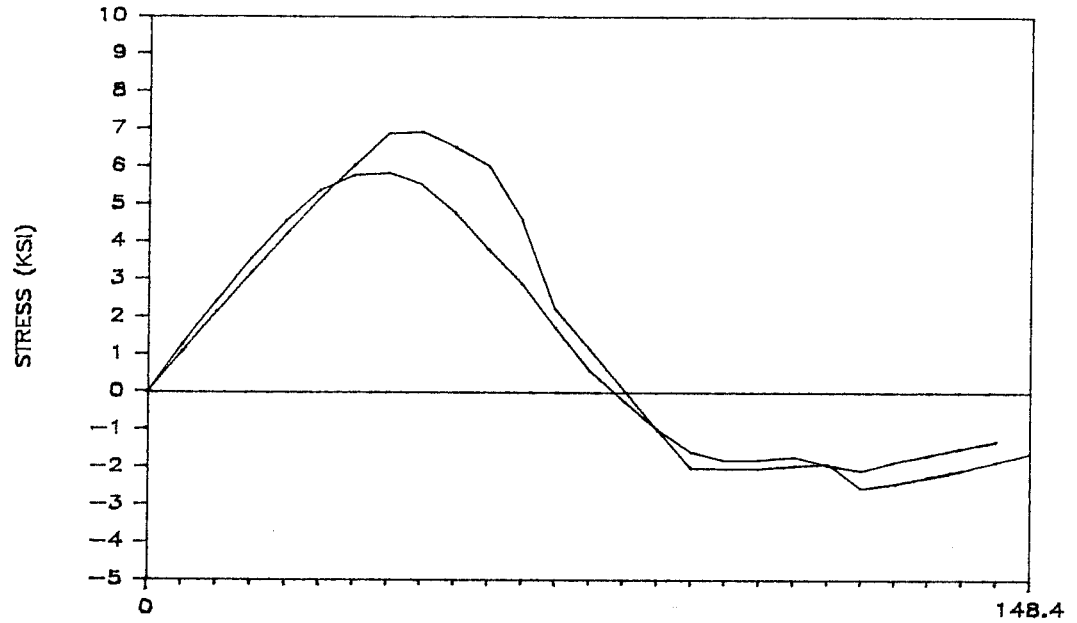

4.16

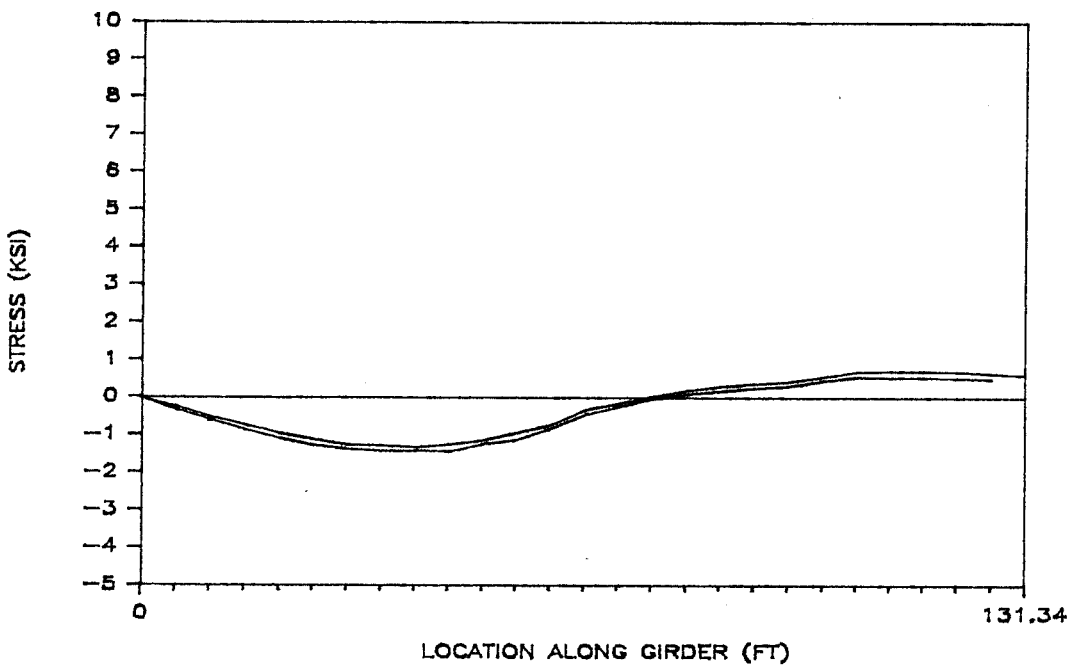

Outer

B1, G1&4

~~4.18~~

4.17C

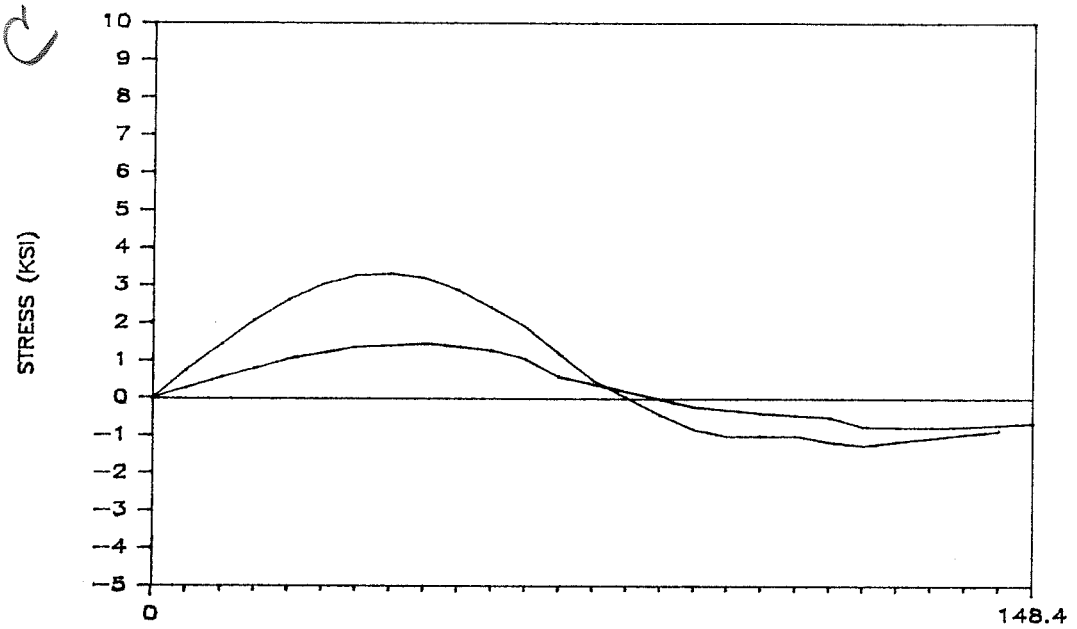

4.18D

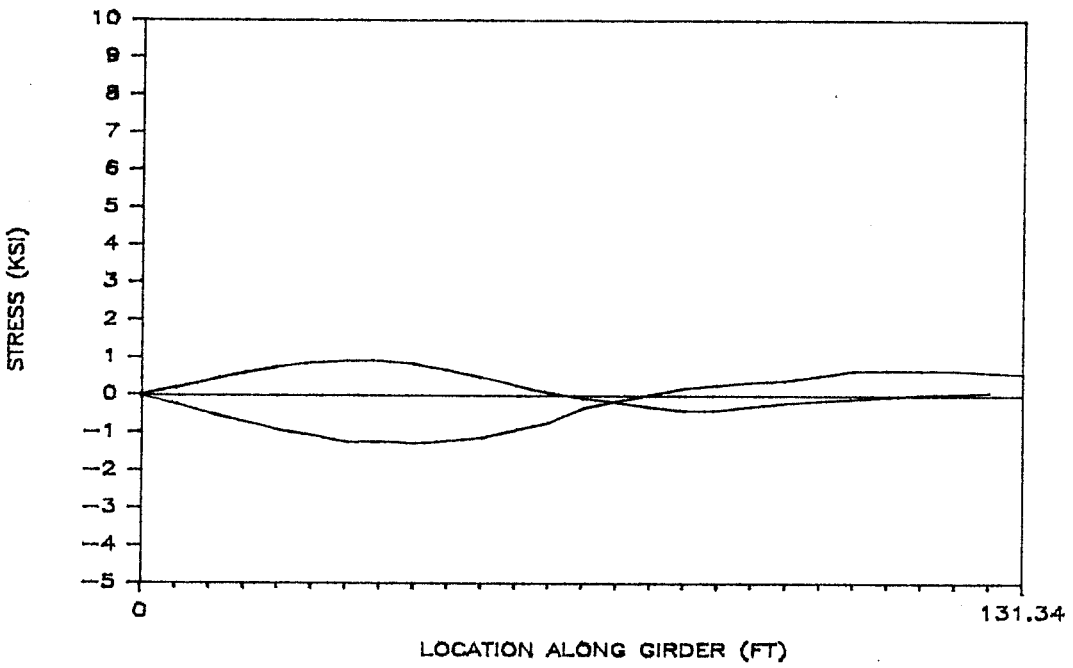

Middle

4,18a

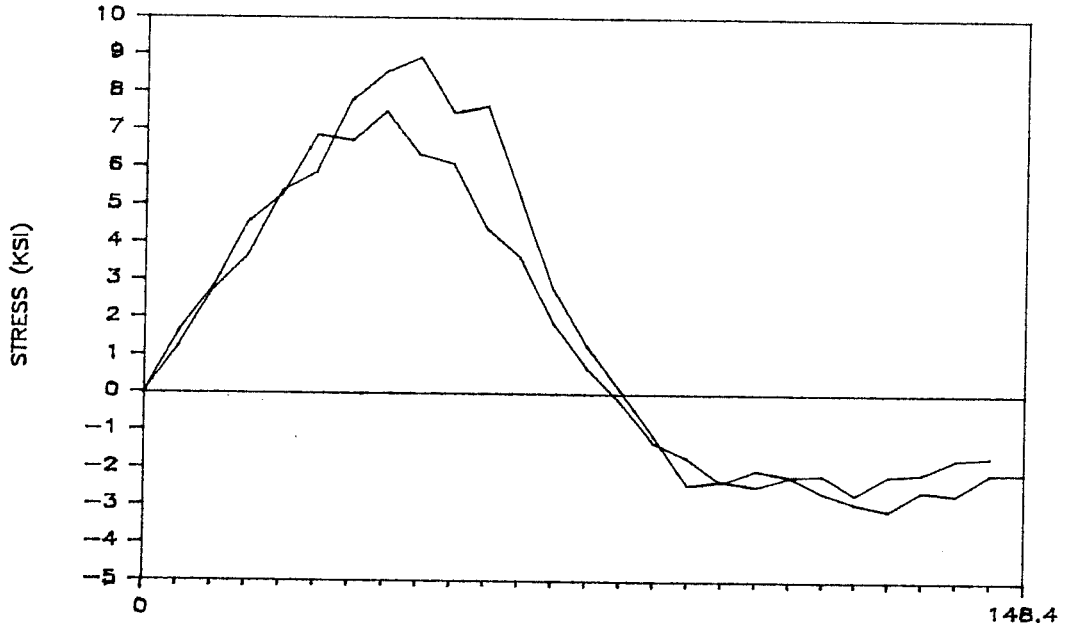
STRESS (KSI)
10
9
8
7
6
5
4
3
2
1
0
−1
−2
−3
−4
−5
0
148.4

4,18b

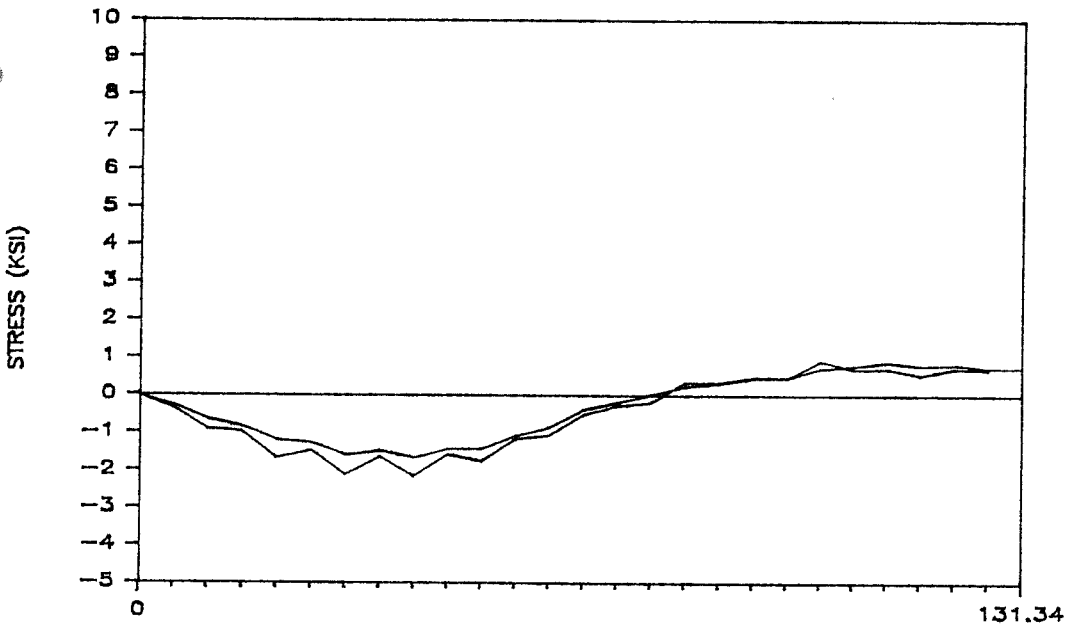
STRESS (KSI)
10
9
8
7
6
5
4
3
2
1
0
−1
−2
−3
−4
−5
0
131.34

4.18dc

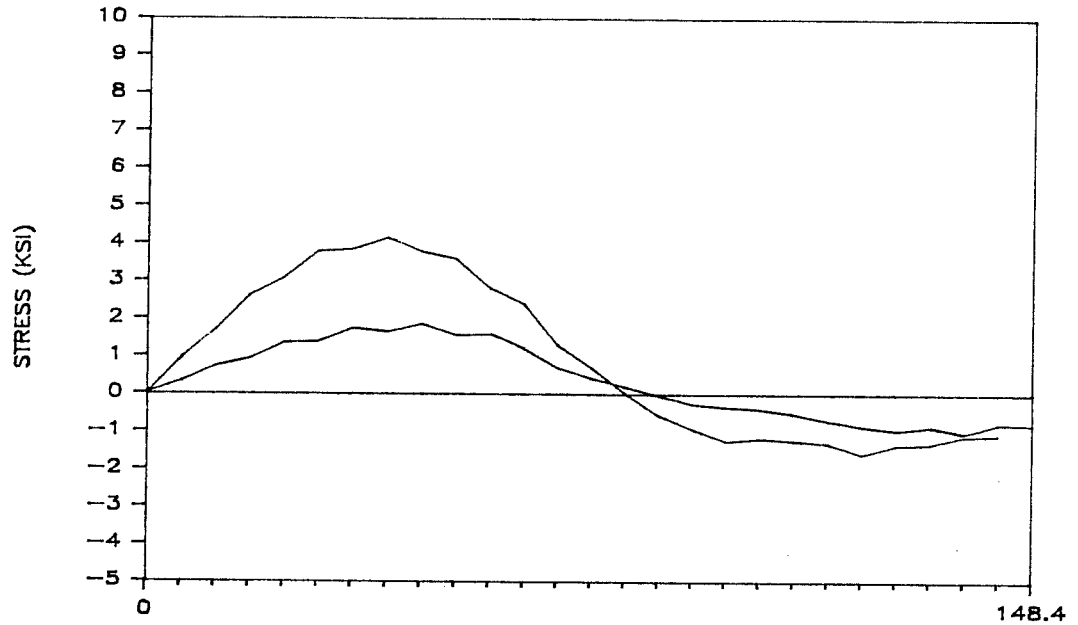
STRESS (KSI)
10
9
8
7
6
5
4
3
2
1
0
−1
−2
−3
−4
−5
0
148.4

4.18d

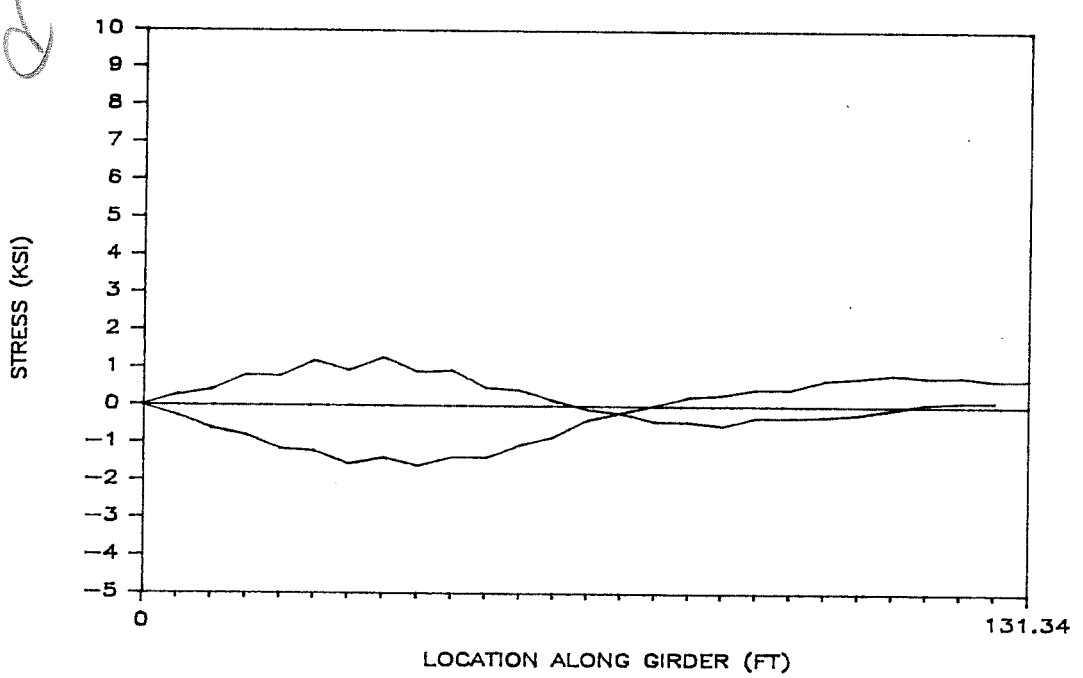
STRESS (KSI)
10
9
8
7
6
5
4
3
2
1
0
−1
−2
−3
−4
−5
0
131.34
LOCATION ALONG GIRDER (FT)

4.19a

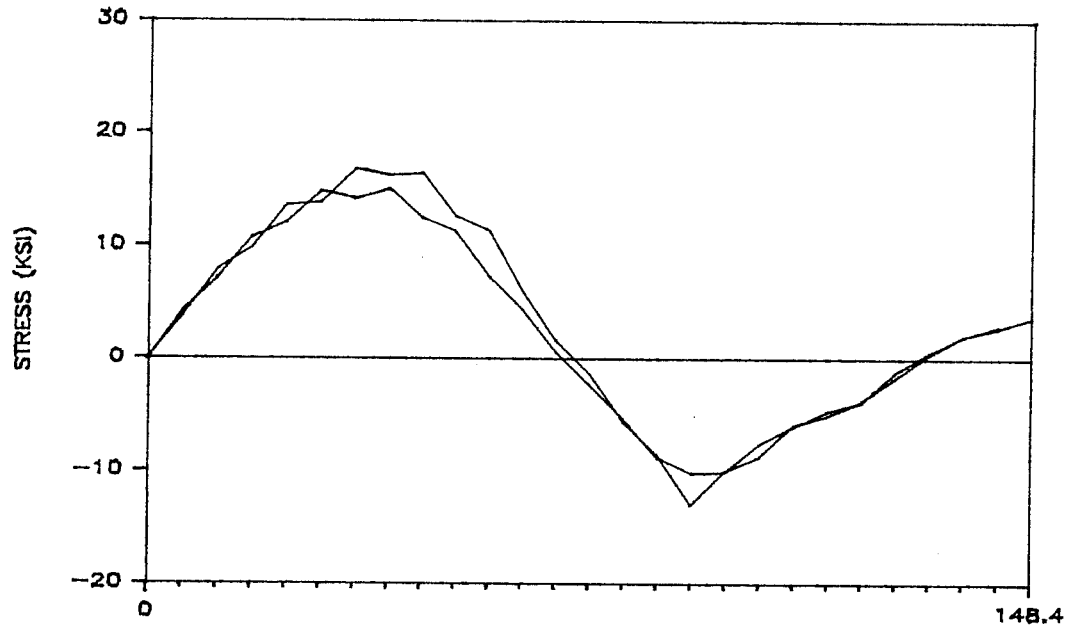
30
20
10
0
−10
−20
STRESS (KSI)
0
148.4

4.19b

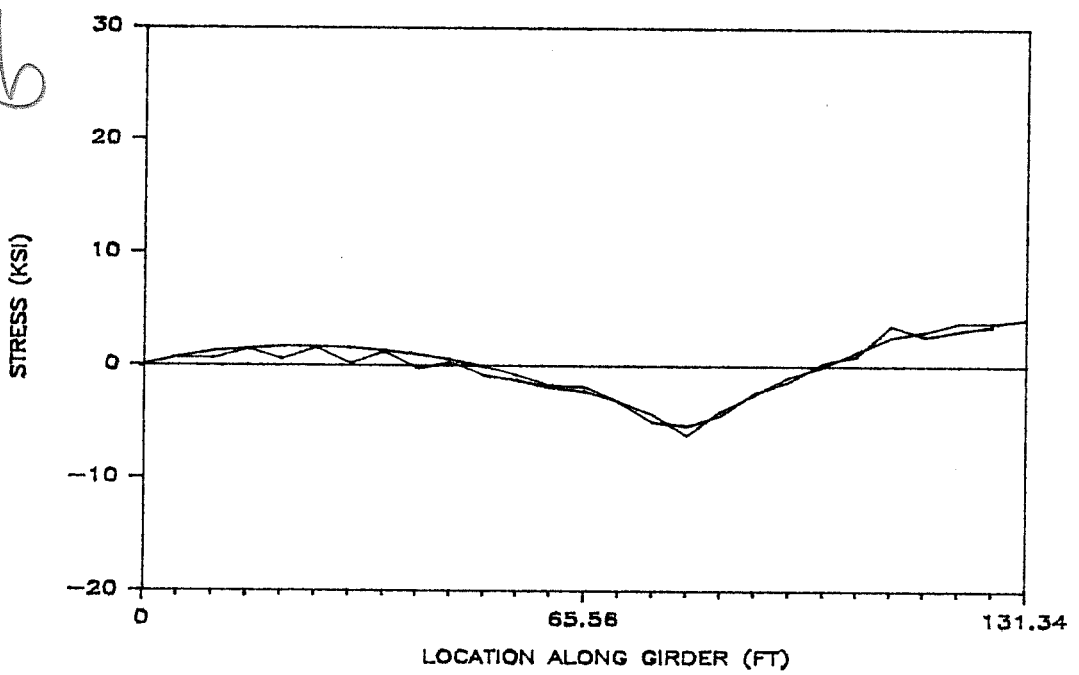
30
20
10
0
−10
−20
STRESS (KSI)
0
65.56
131.34
LOCATION ALONG GIRDER (FT)

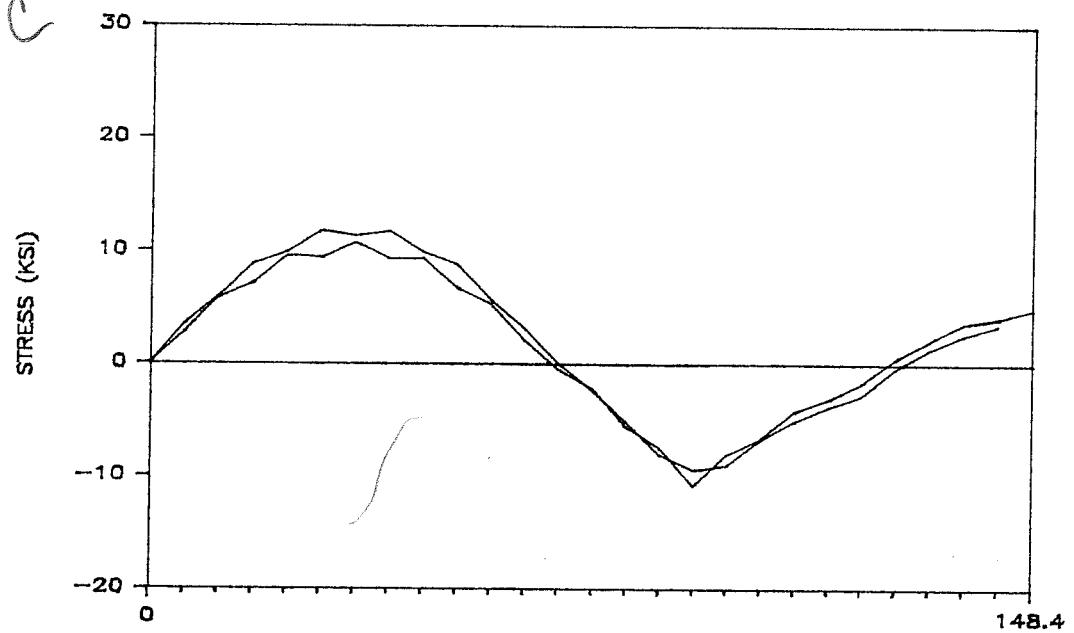
30
20
10
0
−10
−20
STRESS (KSI)
0
148.4

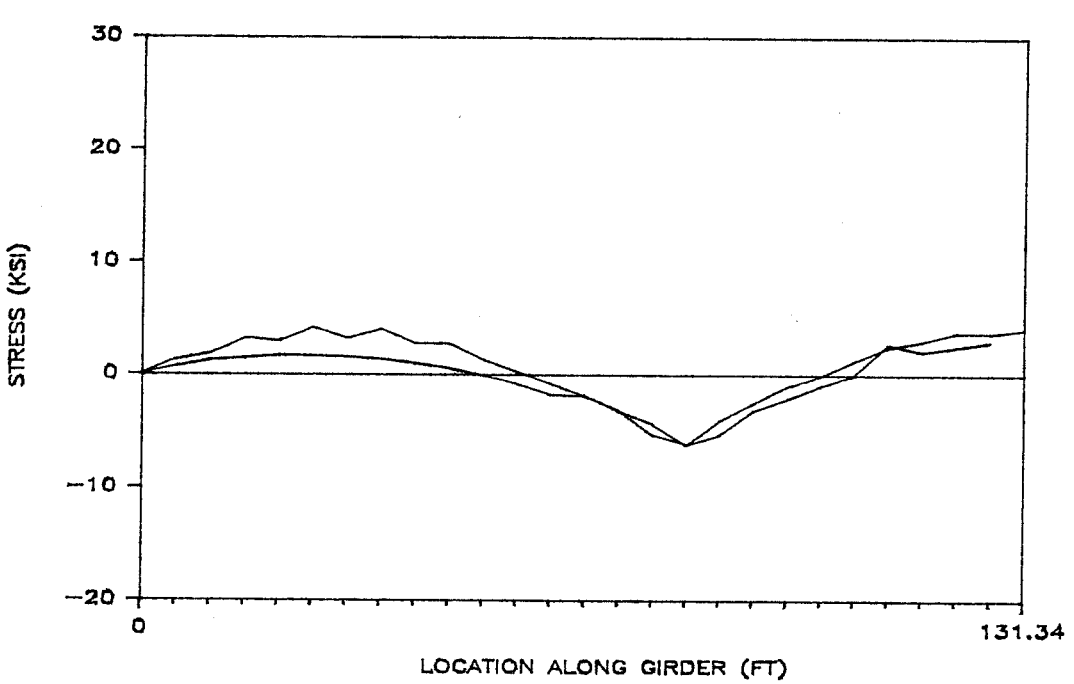
30
20
10
0
−10
−20
STRESS (KSI)
0
131.34
LOCATION ALONG GIRDER (FT)

4.21a

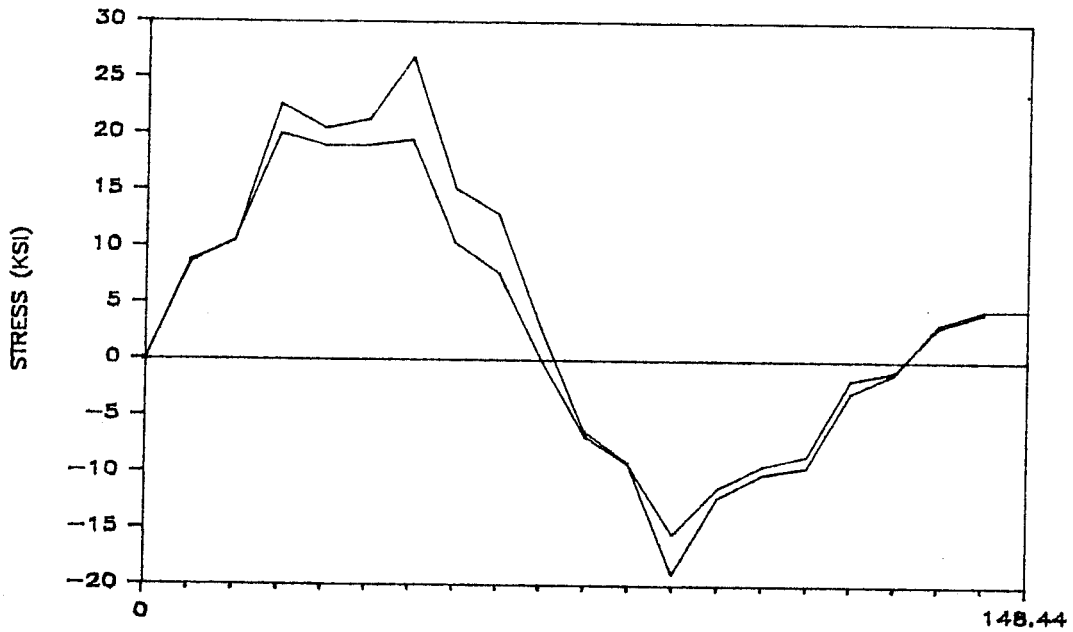
30
25
20
15
10
5
0
−5
−10
−15
−20
STRESS (KSI)
0
148.44

4.21b

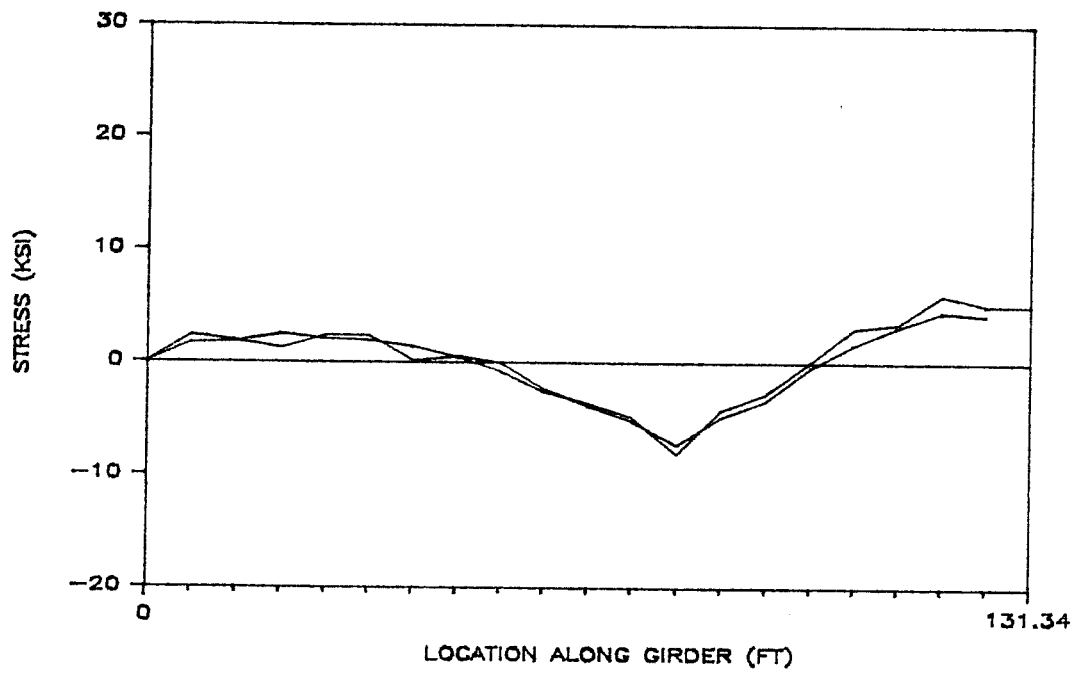
30
20
10
0
−10
−20
STRESS (KSI)
0
131.34
LOCATION ALONG GIRDER (FT)

4.21c

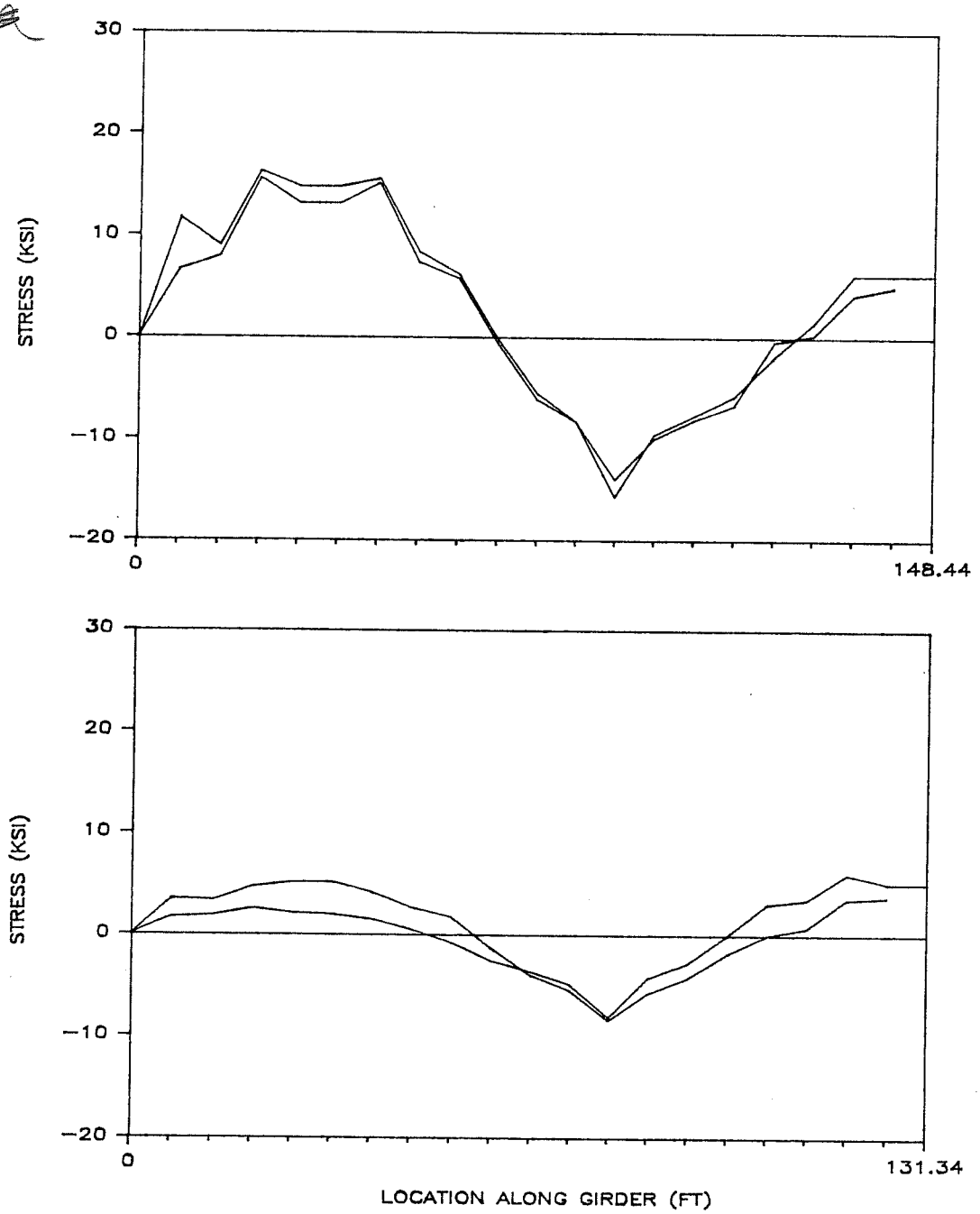
30
20
10
0
−10
−20
STRESS (KSI)
0
148.44
30
20
10
0
−10
−20
STRESS (KSI)
0
131.34
LOCATION ALONG GIRDER (FT)

4.2a

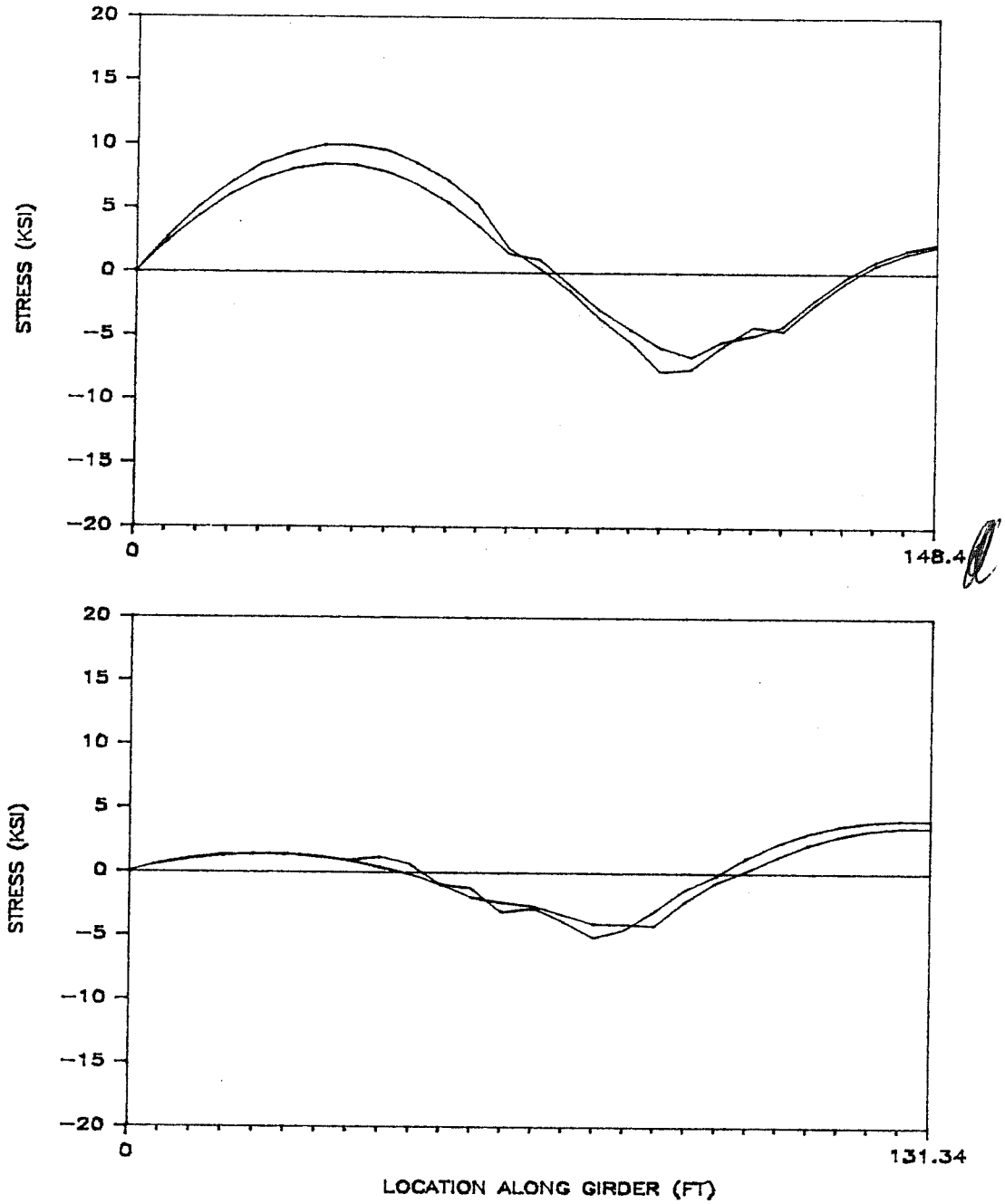
20
15
10
5
0
−5
−10
−15
−20
STRESS (KSI)
0
148.4
20
15
10
5
0
−5
−10
−15
−20
STRESS (KSI)
0
131.34
LOCATION ALONG GIRDER (FT)

4.259

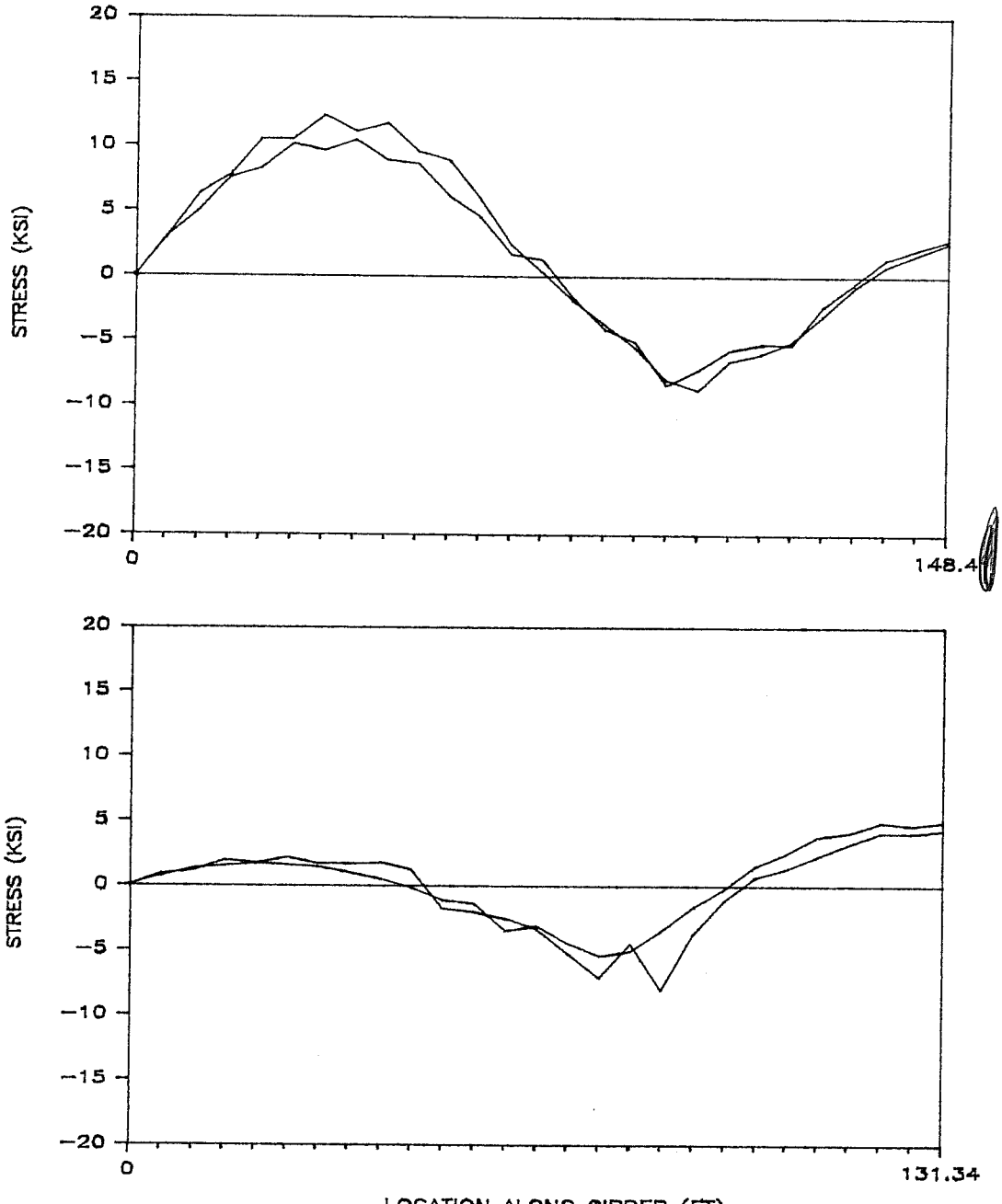
20
15
10
5
0
−5
−10
−15
−20
STRESS (KSI)
0
148.4
20
15
10
5
0
−5
−10
−15
−20
STRESS (KSI)
0
131.34
LOCATION ALONG GIRDER (FT)

ANALYSIS OF HORIZONTALLY CURVED GIRDER BRIDGES

APPROVED:

_____

_____